UC San Diego

UC San Diego Electronic Theses and Dissertations

Title

Development of Probabilistic Algorithms for Unobtrusive Sleep Monitoring Using Epidermal Electronic System : : A Pilot Study

Permalink

https://escholarship.org/uc/item/8b49s71q

Author

Vijayan, Varsha

Publication Date

2014

Peer reviewed|Thesis/dissertation

eScholarship.org Powered by the California Digital Library
University of California

UNIVERSITY OF CALIFORNIA, SAN DIEGO

Development of Probabilistic Algorithms for Unobtrusive Sleep Monitoring Using Epidermal Electronic System – A Pilot Study

A Thesis submitted in partial satisfaction of the requirements

for the degree Master of Science

in

Bioengineering

by

Varsha Vijayan

Committee in charge:

Todd Prentice Coleman, Chair
Mary Jo Harbert
Pedro Jo Cabrales

2014

The thesis of Varsha Vijayan is approved, and it is acceptable in quality and form for publication on microfilm and electronically:

_____

_____

_____

Chair

University of California, San Diego

2014

To Amma, for awakening me to the most important dimension of life, the society.

To Appa, for exhorting me to pursue science.

To Mama, for always being my guiding light.

To all research volunteers of this study for your scientific curiosity.

To strangers who indulge in random acts of kindness & generosity.

Last but not the least –

Posthumously to Manoj Niranjan sir, for teaching us fundamental signal processing courses and for being an epitome of dedication.

TABLE OF CONTENTS

LIST OF ABBREVIATIONS

PSG	Polysomnography
EEG	Electroencephalography
EOG	Electrooccculography
EMG	Electromyography
ECG	Electrocardiography
EES	Epidermal Electronic System
HMM	Hidden Markov Model
EM	Expectation – Maximization
MAP	Maximum a Posteriori
PMF	Probability Mass Function
REM	Rapid Eye Movement
NREM	Non-Rapid Eye Movement
R & K	Rechtschaffen and Kales
PTSD	Post-Traumatic Stress Disorder
TBI	Traumatic Brain Injury

LIST OF FIGURES

Chapter – 2

Chapter – 3

Chapter – 4

Chapter – 5

Chapter – 6

LIST OF TABLES

ACKNOWLEDGEMENTS

This research project would not have come to fruition without the support of a number of people. Although words can only get us so far, all I have here, is just words, to express my deep sense of gratitude, first and foremost to my advisor, Professor Todd Coleman for – helping me get started and involved in the emerging field of data analytics, providing mathematical nudge, being a constant source of encouragement, a repository of epiphanic ideas, positivity and hope. I worked on this project in close collaboration with Dr. Cheolsoo Park who instilled in me, the restless enthusiasm to develop the algorithm, to collect EEG data and to use signal processing techniques for analysis. Dr. Julie Onton at the Naval Health Research Center was instrumental in setting up the experimental design framework based on her long-term experience in performing sleep recording on patients with Post Traumatic Stress Disorder. Dr. Sanggyun Kim provided insightful comments and constructive criticism to mould some of the existing techniques in addition to giving valuable future directions to this project. I would like to thank all my committee members, Dr. Pedro Cabrales, Dr. Mary Harbert and Dr. Piyush Patel – for spending time with me and giving valuable inputs. Dr. Sheila Rosenberg was always there to support me and enabled me to inculcate the moral and ethical qualities of a scientific researcher. Dr. Rui Ma helped me get started with understanding the experimental framework in alignment with the terms of interest for our Neural Interaction Lab at UCSD.

The next layer of support was provided by my ever-friendly labmates. I am fortunate to have experienced familial ties with all of them – Mridu, Marianne, Marcela, Armen (for always fixing the printer as well!), Diego, Hidahis, Yun Soung, Dae, Nicole,

Justin, Alison, Mike, Gladys, Cheryl, Teryn, Amanuel, Gino, Amr, Keerthiga, Victoria. I would also like to thank Dr. Michelle Ferrez, Gennie, Melinda and all transfer students as part of the IDEA Student Center at UCSD. I would also like to thank all of my undergraduate professors & classmates for providing an intellectually stimulating atmosphere which served as a motivation for me to pursue graduate studies.

This section would be incomplete if I don't mention the immeasurable confidence that my family and friends have in me. Usha, Venmathi, Abhirami, Aishwarya, Amal, Priyanka, Aswin, Lakshmi Dhevi, Vineet, Radheshyam, Tejaswy, Naresh – thank you all for your presence, support and for keeping me inspired.

ABSTRACT OF THE THESIS

Development of Probabilistic Algorithms for Unobtrusive Sleep Monitoring using Epidermal Electronic System – A Pilot Study

by

Varsha Vijayan

Master of Science in Bioengineering

University of California, San Diego, 2014

Professor Todd Prentice Coleman, Chair

Traditional sleep monitoring involves obtaining a polysomnography which uses a minimum of six channels of electrodes to record the following biosignals – electroencephalography, electrooculography, electromyography, electrocardiography and other channels for measuring respiration. This multimodality physiological monitoring poses a lot of discomfort for the person undergoing sleep recording and disrupts the natural sleep owing to the bulk of electrodes and wires used for acquiring the signals, in turn defeating the purpose of monitoring sleep as it naturally occurs. Using a novel, thin, flexible Epidermal Electronic System, unobtrusive sleep monitoring can be performed. Ten healthy adults underwent concurrent sleep EEG recording with epidermal electrodes and

conventional electrodes to perform a pilot study, to characterize how similar the clinically relevant aspects of sleep EEG are under the two different recording technologies. Time – frequency spectrogram estimates that can balance temporal and spatial resolution required to understand the EEG acquired from different electrode technologies have been developed. Hypnograms have been generated using state-space probabilistic modeling of sleep EEG from epidermal and conventional electrodes. The outputs of the sleep staging estimators are compared using probabilistic clustering algorithms that operate on the estimates. The outcome of our research demonstrates the capability of epidermal electrodes that can potentially be used as an acquisition cum analysis screening tool for sleep disorders.

Chapter 1 – Introduction

1.1 Motivation

Sleep disorders are becoming a global epidemic. According to research led by Warwick Medical School, an estimated 150 million adults are suffering from sleep disorders in the developing world [1-1]. Exclusively in the US, a CDC survey has estimated that about 50-70 million adults suffer from chronic sleep and wakefulness disorders [1-2]. The economic burden of this issue is around $15.9 billion annually [1-3], in addition to another $100 billion or more of indirect costs involved in property destruction, litigation, hospitalization and death resulting from sleep disorders and sleep deprivation. These estimates clearly show the magnanimity of the problem and why we should be moving towards tackling it. If left unsolved, the problem of sleep disorders can adversely affect the productive lives of the active, working population of the world in addition to a host of other problems that come along.

For uncovering sleep disorders, the principal diagnostic tool in clinical practice is polysomnography. It refers to the continuous monitoring of various neurophysiological and cardiorespiratory variables, over the course of a night for studying normal and disturbed sleep patterns. Electroencephalographic, electrooculographic and electromyographic monitoring provide the basis for staging the epochs (30-second time windows) of signals into wakefulness and various sleep patterns. In addition to the 3-modalities of recording mentioned above, there are other channels of sensors and electrodes for detection of airflow at the nose and mouth by means of thermistors. Analysis of breathing patterns is performed by signals recorded from sensors placed around the ribcage and abdomen. In addition, pulse

oximetry, the electrocardiogram and the combined application of several other measurement techniques allow the assessment of normal and abnormal physiological events in relation to sleep structure. People typically visit exclusive sleep labs that have been designed for the purpose of conducting a polysomnography test. About 1 million such sleep studies are conducted every year, all of which involve the usage of cumbersome and unwieldy instruments attached all over the body of the patient, which inevitably disrupts the normal sleep pattern [1-4]. Indeed, sleep research protocols routinely require two nights of recordings, with the first night not scored because of the issues related to sleep disruption from wearing the sleep equipment. This is known as the first-night effect. Also, conventional polysomnography is expensive, time-consuming, labor-intensive and sleep labs have long waiting lists for overnight PSG studies [1-5]. Apart from this, the sleep scoring schematic for PSG is mostly manual. An expert clinician (somnologist) manually looks at the multi-channel recording and assigns a sleep stage to each epoch according to R&K methodology or rules framed by AASM. This technique, in addition to the disadvantages mentioned above, is subjective and in the presence of multiple scorers is prone to significant inter-scorer variability [1-6, 1-7]. Automatic sleep scoring techniques have been in research for over four decades [1-8]. Most of these are computer-assisted manual scoring methodologies. Existing commercial PSG scoring software tools have neither been tested nor verified upon wide population – that is healthy or has chronic sleep disorders. An added problem is that there is a lack standard methodology to compare the different sleep scoring software tools as the approach followed by each of these algorithms is different.

Hence, there is a persisting need for an easy-to-wear, portable system that can perform sleep monitoring unobtrusively. The system must also give a read-out of objective sleep scoring that can been used by healthy human population in addition to those with chronic sleep disorders.

In this thesis, the capabilities of novel, flexible electronic tattoos (epidermal electrodes) are tested for the purpose of sleep monitoring. Simultaneous sleep EEG data collected from 10 subjects is analyzed and hypothesis testing is performed on the data. Hidden Markov model based probabilistic modeling is employed to automatically estimate the sleep staging. The results of modeling and hypothesis testing indicate that epidermal electrodes could be a promising alternative to conventional electrodes as a seamless sleep monitoring device that comes along with powerful analytics for objective sleep scoring.

1.2 Organization of the thesis

Chapter 2 gives an overview of the background of sleep physiology and relevant literature review of previous experimental studies. Chapter 3 deals with the description of the materials and protocols used in this project. The mathematical framework of the thesis is covered in chapter 4. The results of hypothesis testing are shown in chapter 5. Discussion, conclusion and future directions are part of chapter 6.

Chapter 2 – Background

2.1 Sleep Architecture

The basic structural organization of normal sleep is called the sleep architecture. There are two main types of sleep – non-rapid eye movement (NREM) and rapid eye movement (REM). NREM sleep is divided into stages 1, 2, 3 & 4 according to R&K. Stages 3 & 4 were recently combined into a single stage 3 by AASM in 2007 [2-1]. Each sleep stage has unique characteristics of variations in electroencephalography (brain waves), electrooculography (eye movements) and electromyography (muscle tone). As sleep is primarily a neural process, observation of brain activity has been the key aspect of uncovering sleep cycles. This has been done through the characterization of changes using electroencephalographic (EEG) recordings that trace the electrical patterns of brain activity. The NREM and REM sleep stages alternate cyclically throughout the night.

A hypnogram is a graph representing stages of sleep as a function of time. Shown below is a hypnogram of a healthy individual's normal night's sleep.

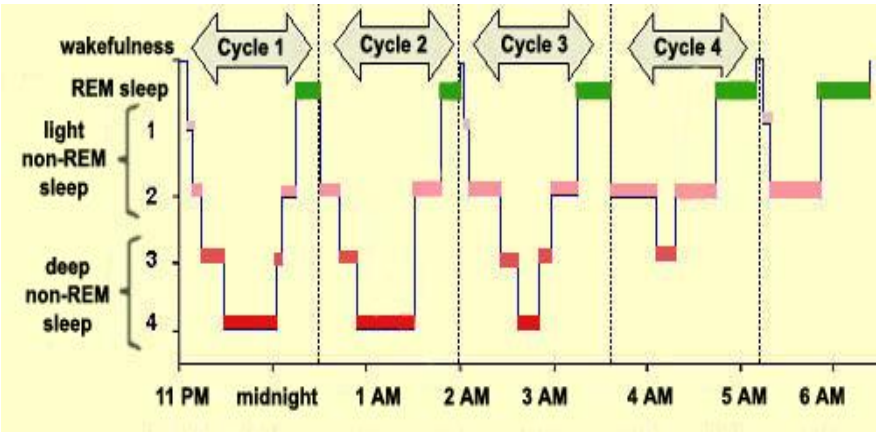

Figure 2.1: Hypnogram of healthy subject's normal sleep architecture [2-2]

2.2 Sleep Stages

This section gives a brief overview of the physiological and electrical manifestations of changes occurring during each sleep stage [2-3, 2-4, 2-5].

2.2.1 Non-Rapid Eye Movement Stage – 1

The transition between being awake and beginning to sleep is represented by NREM sleep stage 1. It lasts 1-7 minutes in the initial cycle, constituting 2-5% of total sleep and is easily interrupted by a disruptive noise or light. This stage is characterized by transition from alpha waves (8-13 Hz) to theta waves (4-7 Hz) of EEG. Slow, asynchronous eye movements may be observed at this stage. Sudden twitches and hypnic jerks may be associated with onset of sleep during this stage.

2.2.2 Non-Rapid Eye Movement Stage – 2

The NREM sleep stage 2 accounts for 45-55% of the total sleep episode. It lasts for a duration of 10-25 minutes in the initial cycle and lengthens in successive cycles. Sleep spindles, which represent periods where the brain is inhibiting processing to keep the sleeper in tranquil state, characterize stage 2. These spindles occur in 12-14 Hz band of EEG. In addition, K-complexes, that suppress cortical arousal to stimulus and promote memory consolidation, also belong to stage 2. Muscular activity measured by EMG decreases, so do the eye movements (EOG).

2.2.3 Non-Rapid Eye Movement Stage – 3

The NREM sleep stage – 3 is also known as slow wave sleep (SWS), most of this stage occurs during the initial duration of the night. In the first cycle, this stage lasts for about 20-40 minutes and in subsequent cycles the duration shortens. This stage has

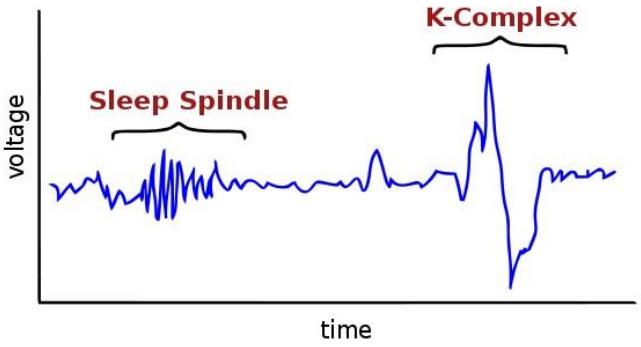

Figure 2.2: A fictional EEG showing a sleep spindle and K-complex in NREM stage 2 sleep [2-6]

dominant delta wave (0-3 Hz) activity in EEG. EOG and EMG activity are almost absent.

2.2.4 Rapid Eye Movement Stage

The REM sleep stage is characterized by low voltage, high frequency, saw-tooth shaped EEG, rapid eye movements and muscle atonia (extremely relaxed state of skeletal muscles). This stage accounts for about 20-25% of the total sleep duration. During the initial cycle, REM period lasts for only about 1-5 minutes and it becomes subsequently prolonged as sleep episode progresses. Vivid dreams occur during this stage. Since the physiological parameters of REM sleep stage resemble that of normal, waking counterparts, this is also referred to as paradoxical sleep.

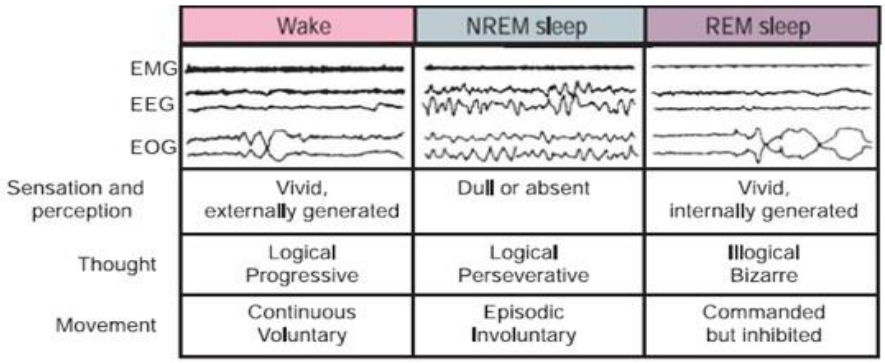

Figure 2.3: Behavioral states during different phases of sleep [2-4]

2.2.5 Sleep Cycles

NREM stage 1 marks the beginning of a sleep episode. It progresses through to stages 2, 3 and finally to REM after which the same pattern of cycling continues throughout the night until the person wakes up. NREM sleep constitutes about 75-80% of total time spent in sleep while REM sleep constitutes about 20-25%. In a healthy adult, REM sleep duration increases as the night progresses and is the longest in the last one-third of the sleep episode. An opposite trend is observed in the case of deep sleep (stage 3). As the sleep episode progresses through the night, NREM stage 2 dominates and NREM stage 3 (slow wave sleep) disappears eventually.

2.3 Polysomnography - The current gold standard diagnostic tool in clinical practice

Polysomnography (PSG) is the principal diagnostic tool in clinical practice for uncovering the sleep architecture of a subject. It is a comprehensive recording of biophysiological changes that occur during sleep.

Figure 2.3: A subject undergoing polysomnography recording [2-7]

The polysomnography recording entails monitoring of patients in an exclusive sleep facility using an array of medical equipment. Specially trained sleep technologists perform polysomnography for the diagnosis and treatment of sleep disorders. The standard diagnostic PSG requires the recording and evaluation of sleep stages and arousals, respiration, limb movements, snoring, oximetry, body position, and cardiac rhythm disturbances. Hence, a polysomnogram will typically record a minimum of 12 channels requiring a minimum of 22 wire attachments to the patient [2-8]. The corresponding measurements that are recorded as part of a polysomnography test are a minimum of the following modalities: three channels for EEG, two for eye movements – EOG, one for chin muscle tone – EMG, one each for the belts which measure chest wall movement and upper abdominal wall movement, accelerometer based devices for limb movement, one to measure air flow, one for oxygen saturation and one or two for heart rate and rhythm. This cumbersome multimodality recording, in addition to disrupting the natural sleep rhythm of the subject [2-8], is very expensive. Typically, only a single night or two nights of polysomnography are recorded. Sleep is a very dynamic process; the pattern of sleep

recorded multiple nights is more useful than a single night recording. Multiple recording using PSG is very challenging due to all the disadvantages that it comes with, as mentioned earlier. In light of this, newer portable monitoring devices with reduced number of channels of recording are currently beginning to come to use [2-9]. For instance, some of these devices require only 3 to 4 channels: air flow, pulse oximetry and other respiratory recordings. Because of the absence of EEG, EOG, EMG, these devices do not stage sleep according to electrophysiological protocols (of AASM): they are exclusively used only for screening for sleep apnea, leaving out other sleep disorders. In addition to portable monitors with reduced number of channels, the technique of actigraphy [2-10] has been used as an alternative to PSG. It is an objective, indirect measurement of sleep and wakefulness. It uses movement as a substitute for wakefulness and hence, is prone to misinterpreting quiet wakefulness as sleep. The commercially available movement-based sleep monitoring devices are Actiwatch – 64, Fitbit, Jawbone UP to name a few. The demerits of these different sleep recording methodologies has led to research in devices that use only single – channel EEG.

2.4 Literature Review

Shambroom et al. [2-11] performed a validation study of a single-channel frontal EEG (approximately, Fp1-Fp2) based wireless sleep monitoring system by collecting time-synchronized sleep data simultaneously using their system along with PSG and actigraphy (ACT). The study was conducted on 29 healthy volunteers. Their wireless system (WS) used proprietary dry silver-coated fabric sensors in a headband to collect signals from single bipolar channel Fp1-Fp2. The collected electrophysiological signals included

contributions from EEG, EOG and frontalis muscle EMG. The best estimate of the sleep score using their wireless system was based on R&K method of scoring, which is calculated from the recorded EEG signal using an artificial neural network that uses time and frequency dependent features. The sleep stage is reported every 30s (1 epoch). A reduced set of sleep stages including wakefulness, light (stage 1 & 2), deep (stage 3 & 4) and REM, were reported. Epoch – by – epoch agreement between two PSG scorers and the wireless system was evaluated – (PSG1 vs. WS, PSG2 vs. WS) and (PSG1 vs. PSG2). WS agreement with each of the two PSG scores for sleep/ wakefulness was 92.6% and 91.1%, ACT agreement with PSG was 86.3% and 85.7%. The PSG scorers' agreement with each other for sleep stages was 83.2%, and for sleep/ wakefulness was 95.8%. The findings of this validation study indicate that the single-channel EEG based WS may provide an easy to use and accurate complement to other established technologies for measuring sleep in healthy adults.

D. Popovic et al. [2-12] performed a validation study investigating the accuracy and limitations of automatic sleep scoring and EEG arousals in Fp1-Fp2 montage. 29 healthy adults underwent the study in which the scalp EEG (C3–A2, C4–A1, Fz–Oz, Cz–Oz), left and right EOG, submental EMG, the Fp1–Fp2 signal and the signal from a respiration belt were acquired using an ambulatory PSG recorder. The forehead electrodes were placed on the frontal eminences, approximately 1 cm laterally from the Fp1 and Fp2 positions of the 10–20 system. The algorithm performs spectral decomposition of the input signal, computes descriptors of sleep macro and microarchitecture, performs artefact detection and classifies 30-s epochs into one of the five stages – wake, REM, NREM1, NREM2, NREM3. Of the total number of recordings, about 10 subject recordings were

chosen for training the algorithm and the rest were used for validating the algorithm. The scoring of the validation group was done at five levels: (i) by a referent scorer in accordance with AASM guidelines, (ii) by the same scorer blinded to the data for rescoring only Fp1-Fp2 recording 6 months later, (iii) by the same expert scorer who rescored all the recordings in the data 1 year later, (iv) by another expert scorer who observed AASM rules and (v) by the automatic algorithm. The agreement between the algorithm and reference scoring (81%) was comparable to the between inter-rater agreement (83%) or agreement between referent scoring and rescoring of only the frontopolar derivation 6 months later (80.7%). The findings of this research work validate the efficacy of automatic scoring of sleep stages and arousals using just single frontopolar channel EEG as method of assessing sleep architecture in healthy adults.

The two research studies outlined above, show the potential of using single-channel EEG for long-term sleep monitoring. Our research, as part of this thesis, is motivated by the above mentioned studies for frontopolar EEG signal acquisition and automatic sleep scoring.

Chapter 3 – Materials & Protocol

The principal sleep monitoring diagnostic tool, polysomnography is unwieldy and it disrupts the natural sleep, defeating the purpose of sleep monitoring in itself as mentioned in the previous chapters. The novel epidermal electronic system based sensors developed in our lab has features that indicate to be a promising alternative to the existing electrode system. In this pilot study, we simultaneously recorded single – channel sleep EEG from two different technologies of electrodes, namely, conventional electrodes and epidermal electronic system from the same forehead location by placing the electrodes in close proximity to each other. The reason behind performing the study is to test our hypothesis of whether epidermal electronic system and conventional electrodes record similar EEG signals for sleep monitoring.

3.1 EEG Sensing and Recording Equipment

3.1.1 Electrodes

This electrodes under investigative comparison in the study are epidermal electrodes and conventional pre-gelled Ag/ AgCl electrodes.

3.1.1.1 Epidermal Electronic System

The epidermal electronic system (EES) has remarkable advantages of being extremely low profile and thus less likely to impact sleep quality negatively during recording. The development of EES has been described in the Science paper “Epidermal Electronics” [3-1]. The EES conforms to the contour of the human epidermis, and can be

used to record electrophysiological activity such as electrocardiography (ECG), electromyography (EMG), electroencephalography (EEG), electrooculography (EOG). The EES is a very slim, comfortably worn, non-invasive device. Flexibility and stretchability, the key mechanical properties inherent to the EES device, enable it to stick to the skin. All materials of the EES that contact the skin are biocompatible and consist of elemental gold, polyimide and silicone. In the work that originally introduced the EES, Dr. Coleman's group found that the EES could be worn for 24 hours without irritation of the skin or degradation of the data from the device. This is particularly relevant for sleep monitoring that requires the EES to be left on the skin for long hours. The unique mechanical characteristic of the devices (total thickness < 300 um, total weight < 0.09 g) enable them to be easily laminated onto the skin, and conform to the contours of the skin.

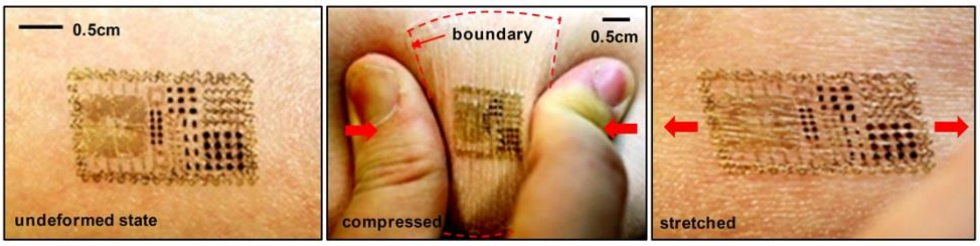

Figure 3.1: Epidermal Electronic Sensors (EES) - is mechanically invisible to the user wearing it, like a temporary tattoo. It is ultra-thin (< 300 um), ultra-light (< 0.09 g) and deforms with the skin.

3.1.1.2 Conventional Electrodes

The conventional electrodes are pre-gelled silver-silver chloride (Ag/ AgCl) electrodes. For the initial 11 out of the 14 subjects recruited for this experimental study, GS26 pre-gelled disposable sensors were used. It has a snap-on 10mm sized sensor pellet, pre-gelled with a 0.5% saline based gel and embedded into a paper thin, clear adhesive disc. This electrode has about 1-inch outer diameter [3-2]. This particular conventional

electrode was chosen because of its small size and ease of application in the relatively less exposed skin area available in the mastoid region. However, the shelf-life of these electrodes was observed to be less than 2 months, since the recordings that were performed after that duration were observed to be of poor quality. Because of the deteriorated signal quality beyond the expiration date of the electrode and lack of rigorous skin prep of the subject, 3 of the 14 recordings could not be included in the study.

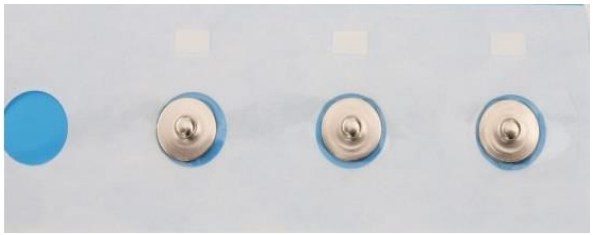

Figure 3.2a: GS26 pre-gelled Ag/ AgCl electrode

Figure 3.2b: Ambu BlueSensor N pre-gelled Ag/ AgCl electrodes

For the final 3 out of 14 subjects recruited for the recordings used for arriving at an inference, Ambu ® BlueSensor N was used as the conventional electrode (shown in Figure 3.2b). The dimensions of the measuring area of the sensor material is about 95 mm^2, which is comparable to the sensor previously used. It has features including highly conductive wet gel, offset connector and superior adhesion for medium-term application and with comfortable foam backing, the electrode is easy to use and gentle to the skin [3-3].

At a high level, Figure 3.3 shows a comparison plot indicating the level of performance measurement of our epidermal electronic system (with and without analytics) with respect to the existing electrodes.

3.1.2 Avatar EEG Recorder

Each of the two types of electrodes were connected to a separate portable, pocket-sized, eight channel EEG recorder known as Avatar EEG. This recorder has a removable memory card with 8GB-32GB capacity that can store weeks of recording

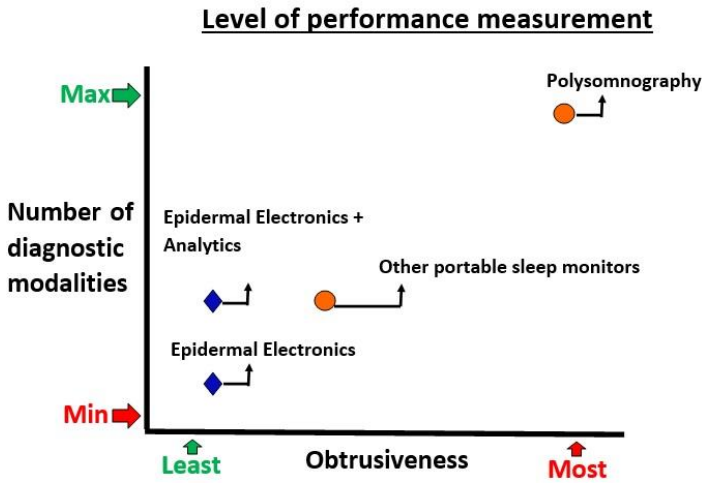

Figure 3.3: Comparing the level of performance measurement of epidermal electronic system.

of signals for offline analysis and can be used for over 24 hours of continuous recording without battery draining problems [3-4]. The recorder also has provision for software configurable gain adjustment. It weighs 60 grams and has dimensions of 76X53X38 mm. The sampling rate was set to 500 Hz. In order to have an unbiased, simultaneously parallel recording of sleep EEG from two different sensor electrodes, two separate recorders were required because each one of the recorder has provision for only a single ground. The recorder is compliant with American Academy of Sleep Medicine (AASM) guidelines for staging sleep and is ideal for sleep studies, post traumatic studies involving sleep and sleep disturbances.

Figure 3.4: Pocket-sized Avatar EEG recorder

3.2 Subject recruitment

Naval Health Research Center (NHRC) Institutional Review Board (IRB) approval was obtained for protocol ID NHRC.2013.0017 titled "Collection of waking and sleep EEG from normal, healthy civilian population for comparison with data from military populations with PTSD and TBI" (abbreviated title – "Normative Waking and Sleep EEG"). The subjects were recruited through word-of-mouth description of the sleep study research that was going to be conducted. After the subjects expressed initial interest and volunteered to participate in the study, a phone call assessment was conducted to check if they satisfied all the inclusion criteria and dissatisfied the exclusion criteria mentioned in the IRB. It was also ensured that subjects participating in the study have no bed partner, or will be able to sleep alone for the nights of the sleep monitoring to minimize artificial sleep disruptions. Self-reporting of the subjects was relied upon for the inclusion/ exclusion criteria.

Inclusion criteria

- Age group 18-50

- Any ethnic background
- Smokers and caffeine-drinkers will be permitted

Exclusion criteria

- Current psychiatric or neurological disorders
- Under medication in the recent 2 years ('medication' refers to chronic use of any prescription substance for mood or physiological regulation, with the exception of birth control)
- Taking or have taken anti-depressants, anti-anxiety or anti-psychotic medication for longer than 1 year in the past and within 2 years of enrolling in the study
- Problems with falling or staying asleep
- A history of skin allergies or a history of extreme sensitivity to cosmetics or lotions
- Using sleep aids such as Ambien or other prescription or over the counter substances, except for rare instances of normalizing sleep during travel between time zones
- Battle field experience

A voluntary consent form was signed by the subjects before beginning the study. In addition, the subjects were given a detailed explanation of the procedures and they clarified their doubts before the experiment began. After signing the consent form, the subjects were given 4 questionnaires that inquired them about their sleep, personality, anxiety, feelings – emotions as well as psychological health. These were: the Patient Health Questionnaire (PHQ-8) for depression, Beck Anxiety Inventory, a personality assessment questionnaire and a sleep quality index questionnaire. After completing the questionnaires, the subjects were given the option of wearing the sleep devices with the help of the researcher or were allowed to observe a demonstration and were given written instructions of how to wear the sleep devices at home. Signatures were obtained for taking a photograph

and/ or video recording of them after wearing the sleep devices – which would eventually be used in paper publications and research presentations. Based on the above outlined procedures, we had recruited 14 subjects for our study, of which only 10 subject recordings were used for making inference. The details on sources of error are given in chapter 6.

3.3 Electrode placement

3.3.1 Skin preparation

The actual preparation for wearing the devices begins with the skin prep. The regions of skin where the electrodes were to be placed were prepped by gently abrading the skin with NuPrep or 3M Red Dot Trace Skin Prep to increase signal clarity by decreasing skin impedance and enhancing signal transmission [3-5]. We avoided using alcohol for skin preparation since it is known to dehydrate the skin causing impedance to rise. A thin layer of conductive, non-irritating, hypoallergenic and bacteriostatic Signa gel [3-6] was applied to the epidermal electrodes before applying onto the skin.

3.3.2 Electrode montage

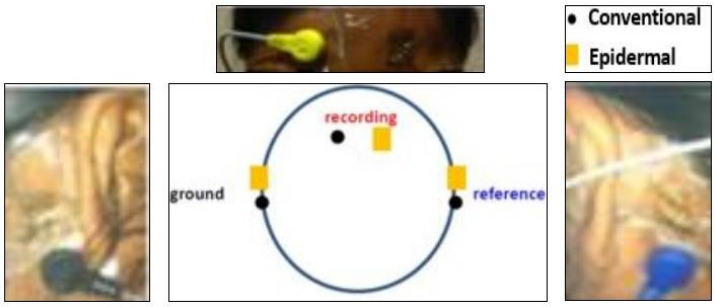

Figure 3.5: Electrode placement on the subject

A total of three Tegaderm (a 3M Health Care product approved for clinical usage) mounted EES stickers were applied on the subject's skin. One EES Tegaderm sticker was

placed on the forehead and two more EES Tegaderm stickers were placed with one behind each ear on the mastoid bone location to record EEG. The reference electrode was placed behind the left ear while the right ear location was assigned to be the ground. In the regions as close as possible (side-by-side) to where EES stickers had been placed, a conventional pre-gelled disposable silver-silver chloride (Ag/ AgCl) surface electrode was applied – to facilitate simultaneous recording from both of the systems. The reason behind choosing mastoid montage was to have ease of application and removal of electrodes in non-hairy areas. The left mastoid reference is commonly used as it provides a location for robust attachment of the electrode with low impedance [3-7]. In addition to that, the mastoid montage framework was also in place for a study at the naval health research center for studying the sleep architecture of PTSD patients. Since this study will eventually evolve into comparing the sleep architectures of healthy subjects vs. those with PTSD, the montage was retained to have mastoid reference.

The subjects were instructed to blink 20 times when they lie down and know they were about to sleep. This is to facilitate synchronization of the epidermal and conventional EEG signals to know where exactly the starting point of sleep recording is.

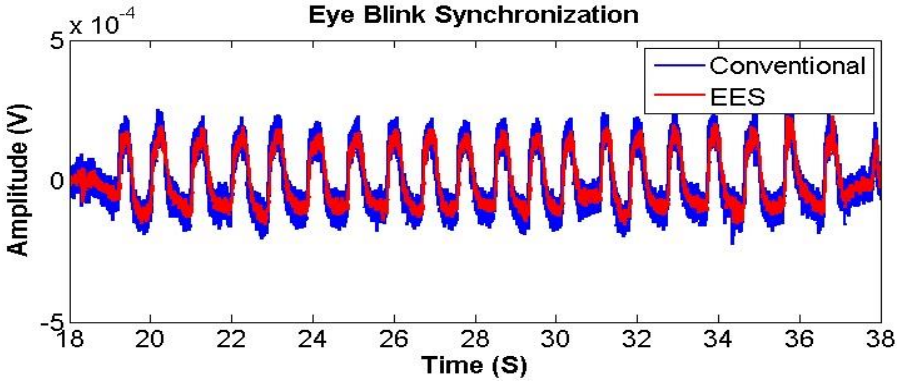

Figure 3.6: Eye blink synchronization signal of one subject

3.4 Overall setup

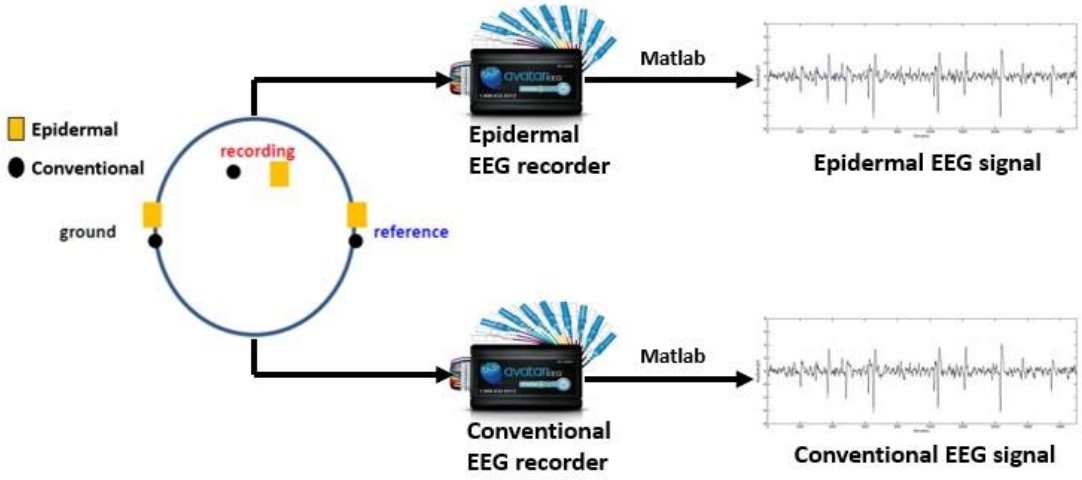

Figure 3.7: Overall representation of acquisition setup

3.4.1 Recording protocol

Full recordings from EES and conventional electrodes were collected on each subject from the instant when the two systems were time synchronized, after which the recording began and the recording continued until the instant in the morning when the subject woke up (the subject ideally had a minimum of 5 hours and maximum of 9 hours sleep). After the subject woke up, EES and conventional electrodes were removed by the subjects themselves. The total duration of the subject's involvement in the study was between 6 and 10 hours for each recording. The subjects were compensated for participating in the study using funding provided by Naval Health Research Center. The EES and conventional electrode sleep data were saved in secure servers in the locked Neural Interaction Laboratory (NIL) at UCSD. Access is password-protected and given only to members of the research team.

Chapter 4 – Probabilistic Modeling

4.1 Signal acquisition and processing

The collected EEG signal was stored in binary data file (.rec) format in the storage memory card of avatar EEG recording device. This file was first converted to .csv file using a python script. The .csv file was then loaded into Matlab software (MathWorks Inc., Natick, MA), and was converted into .mat file.

The sampling rate of avatar EEG recorder was set to 500 Hz. Mean centering was performed to remove any low frequency drift. Due to large size of the data and existing artifacts, the EEG signal was first transformed to capture useful information, as part of the feature extraction process. We employed a technique that used wavelet transforms to extract the power spectral properties of EEG. As the time-frequency decomposition begins, a 2.5s overlapping window, sliding every 0.5s with between-window-shift of 3s, is applied to the raw EEG signal to obtain the localized power spectral density (PSD). Consequently, we have about 7194 data points for every hour of sleep recording. The obtained power values were made non-complex and converted to log-scale (expressed in dB) to normalize the large power differential between low and high frequency power. To minimize the distortions with conversion to dB when power approaches zero, a moving average filter was applied to smooth over every 6 seconds (twice the size of between-window-shift). The line frequency noise was eliminated by using a 60-Hz notch filter. These steps gave rise to f X T power feature matrix with f frequency bins corresponding to 1000 for 0-250 Hz and T time windows depending on the total number of hours of sleep recorded.

In our sleep study paradigm, we define 4 sleep states – wake, REM, light and

deep. NREM stages 1 and 2 have been combined to form a single 'light' sleep stage. Dominant frequency bands corresponding to specific sleep states were defined. We choose n=4 frequency bands: 1Hz-3Hz, 10.15Hz-15.75Hz, 20Hz-30Hz, 35Hz-50Hz, which jointly contain 99% of the power of EEG waves [4-1, 4-2, 4-3, 4-4]. Also, it is well known that human sleep is characterized into different stages based on the frequency content of the delta-wave, theta-wave, alpha-wave, beta1-wave and beta2-wave, which are similar to our frequency bands. Hence, the features contained within these bands should provide enough discrimination power for stage classification [Table 4.1]. However, it is important to note that the frequency band definitions are not universally standardized.

Table 4.1: Dominant frequency bands corresponding to different sleep stages under consideration

Dominant Sleep Stage (Possible X values)	Dominant frequency band (Possible Y values)	Frequency Range (Hz)
Wake (W)	Gamma (γ)	35 – 50
REM (R)	Beta (β)	20 – 30
Light (L)	Sigma (σ)	10.15 – 15.75
Deep (D)	Delta (δ)	1 – 3

Using the extracted power feature, time – frequency spectrogram is plotted. Based on qualitative visual analysis of the spectrogram shown in Figure 4.1, it looks very similar for the conventional and epidermal scenarios. We then go on to build the mathematical framework for sleep staging using the extracted feature from the conventional and epidermal EEG signals.

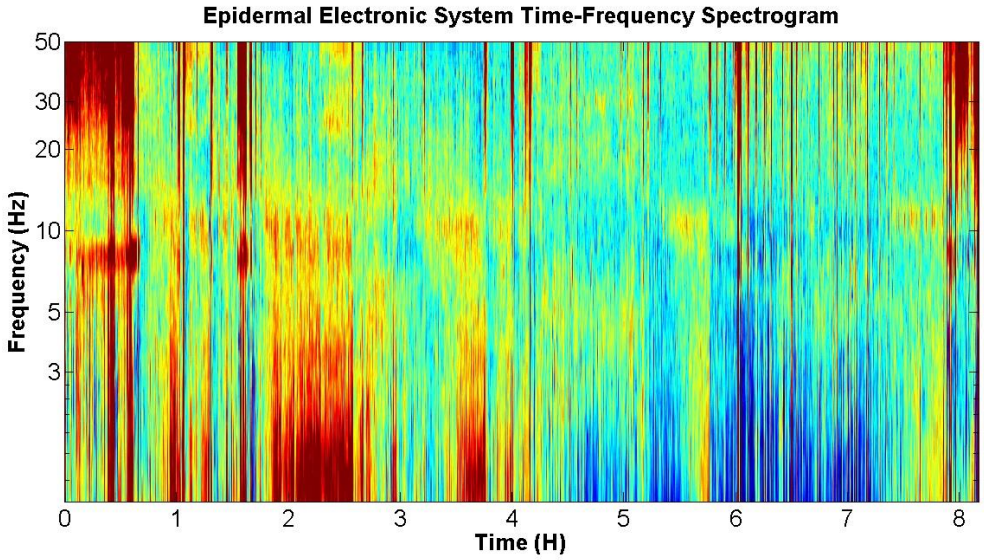

Figure 4.1: Time-frequency spectrogram plot of sleep EEG acquired using epidermal electrode for one subject.

4.2 Markov Process Modeling

Consider X to be a random variable taking on values in some state space (e.g. the discrete values W, R, L, and D pertaining to wake, REM, light, deep). A random process is a collection of random variables indexed through time: $X_i = \{X_1 \dots X_T\}$.

A Markov chain or a Markov process is a random process where the future, X_{i+1} is independent of the past, $X_{1:i-1}$ given the present X_i. The effect of the past on the future is summarized by the state X_i, which changes from one time to the next according to given transition probabilities. In this discussion, the state space is finite. Moreover, we assume stationary transition probabilities (e.g. they do not depend on time). Markov chain models can be applied to any dynamical system whose evolution over time involves uncertainty, provided, the state of the system is suitably defined [4-5].

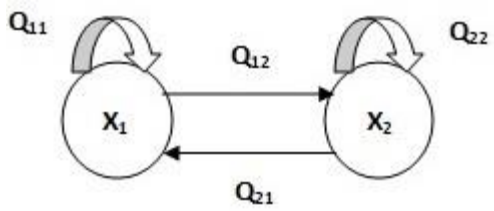

Figure 4.2: A Markov Chain with 2 states labeledX_1, X_2 with selected state transitions.

If $a_1, \ldots a_T$ (for example, $a_1 = 1$, $a_2 = -3$, …, $a_T = 10$) are the values assumed by X_1, …X_T, then, by definition of Markov chain,

$$\mathbf{P(X_i = a_i |\, X_{i-1} = a_{i-1}, X_{i-2} = a_{i-2} \ldots, X_1 = a_1) = P(X_i = a_i |\, X_{i-1} = a_{i-1})} \quad (1)$$

Markov chains can be described by a matrix of state transition probabilities Q whenever the state happens to be a_{i-1}, there is a probability Q that the next state is equal to a_i. Mathematically, this is represented by the equation below,

$$\mathbf{Q(a_{i-1}, a_i) \triangleq P(X_i = a_i | X_{i-1} = a_{i-1}), i \geq 2} \quad (2)$$

$$Q_{ij} = \begin{bmatrix} Q_{11} & Q_{12} \\ Q_{21} & Q_{22} \end{bmatrix}$$

Figure 4.3: Two-state transition matrix

Thus, the probability law of the next state X_{i+1} depends on the past only through the value of the present state X_i. The transition probabilities must be nonnegative and sum to 1.

$$\mathbf{\sum_{j=1}^{n} Q_{ij} = 1 \text{ for all } i} \quad (3)$$

where n represents the total number of possible states.

The initial state distribution, the probability mass function (PMF) on X_1, is given by π

$$\mathbf{\pi(a_1) \triangleq P(X_1 = a_1)} \quad (4)$$

4.3 Hidden Markov Model

A hidden Markov model (HMM) is a statistical model pertaining to two random processes, X and Y, where X is a Markov chain as described above and Y is a "noisy version" of X. In essence, we cannot observe the Markov process $X_{1:T}$ but we can observe another process $Y_{1:T}$ that is statistically coupled to $X_{1:T}$

We describe the coupling of Y to X according to the following definition. At any time i:

$$\mathbf{P(Y_i = b_i | X_{1:T} = a_{1:T}, Y_{1:i-1} = b_{1:i-1}) = P(Y_i = b_i | X_i = a_i) \triangleq R(a_i, b_i)} \qquad (5)$$

This is a fundamental assumption for HMM which means "Y_i is a noisy version of only X_i".

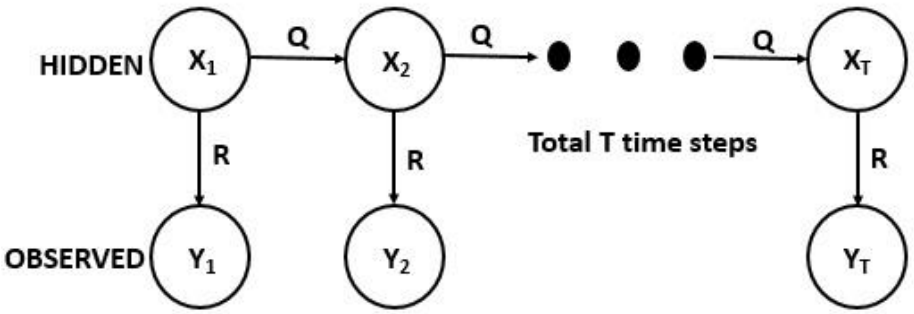

Figure 4.4: Structure of HMM

HMM permits analysis of non-stationary multivariate time series by modeling state transition probabilities (Q) and probability of observation of a state (R). This relates to sleep staging in that: (a) the relationship between the previous sleep stage and next sleep stage obeys a Markov relationship and (b) we do not directly observe the state of sleep; rather, we observe electrical rhythms of the brain that are statistically linked to the

underlying states. As sleep physiology possesses properties of successive stage transition, HMM is a promising model for sleep staging.

4.3.1 Elements of HMM

- **n**: number of states in the model (for example, for sleep, n=4 pertaining to wake, REM, light, deep).
- **T**: total duration of time recorded. T is an integer. For example, we would have $X = \{X_1 = a_1, X_2 = a_2, \ldots, X_T = a_T\}$ where T total time steps and each state at time i, given by a_i, can take one of n values.
- **$\boldsymbol{\pi}$**: initial state probability distribution, that is, $P(X_1 = a_1)$.
- **Q**: state transition probability matrix, that is, $P(X_{i+1} = a_{i+1} | X_i = a_i)$
- **R**: likelihood parameters for $P(Y_i = b_i | X_i = a_i)$

Given appropriate values of n, π, Q and R, the HMM can be used as a generator to give an observation sequence:

$$Y = Y_1\ Y_2\ Y_3\ \ldots\ Y_T$$

The set of {π, Q, R} are collectively referred to as Hidden Markov Model Parameters. The collection is usually denoted by θ, that is, θ = {π, Q, R}.

4.3.2 Sleep Modeling with HMM

Within the context of sleep, hidden random variable (X) represents the sleep stages. X is modeled as a discrete random variable. It can take 4 values corresponding to the defined sleep states according to our sleep study paradigm as shown here:

X: {Wake (W), REM (R), Light (L), Deep (D)}

The continuous random variable Y represents relevant features of the EEG. At any time i, Y_i is a 4-dimensional random variable. The k^{th} component of Y_i, given $Y_{i,k}$, corresponds to the log power in frequency band k from a previous Table 4.1. For example, $Y_{i,1}$ corresponds to the log power in frequency band gamma, $Y_{i,2}$ corresponds to the log power in frequency band beta, etc. We model Y_i as a 4-dimensional Gaussian random variable, whose parameters are given by a 4-dimensional expectation vector and a 4 x 4 covariance matrix.

The most important way to characterize a random variable is through the probabilities of values it can take [4-5]. For a discrete random variable, such as X, these are captured by the probability mass function (PMF) of X. Denote $P_X(a)$ as the probability of the event {X=a}. Analogously, for a continuous random variable, denote $f_Y(v)$ as the probability density of Y at v. For random processes, we index random variables and the associated labels by time. For example, $a_2 = 3$ means that at time unit 2, the sleep stage was in state 3 (corresponding to light) and we denote this probability by $P_{X_2}(a_2)$.

The initial probability distribution represents the probability mass values that the hidden random variable X can take at the beginning of the activity of sleeping, when the subject usually transitions from wake to one of the sleep states. Based on fair assumption, we assign a probability value of 1 to wake stage and 0 to the rest, to start with. The PMF values are assigned in the order of Wake, REM, Light and Deep.

$$\text{Set of states} = \{W, R, L, D\}$$

$$\pi = \{1, 0, 0, 0\}$$

The state transition probability matrix Q represents how probable it is to stay in the same sleep state and/ or transition from one sleep state to another. For short probability durations of time between samples, the probability of staying in the same sleep state is higher than transitioning into other states [4-6]. If there exists a group of states that have low transition probabilities to stay at the same states and high probabilities to transit to each other, the number of states may be higher than necessary for HMM to model the training data [4-6]. A typical value of Q can be obtained from the literature [4-7].

	X = W	X = R	X = L	X = D	
Q =	0.75	0.01	0.24	0	X = W
	0.05	0.88	0.07	0	X = R
	0.18	0.11	0.55	0.16	X = L
	0.02	0	0.14	0.84	X = D

Figure 4.5: Typical value of Q matrix

Mathematically, this can be written as in equation (2). For instance, given that the sleep state at previous time window is wake, the probability that the next sleep state is light is given by the matrix element (1, 3), as in the equation below:

$$\mathbf{Q(1,3) = P(X_L|X_W) = 0.24}$$

Each row represents the PMF values of hidden variable X for one particular sleep stage, so every row adds up to 1. Shown in Figure 4.6 is the PMF for the case when current state is wake (W). The next state could be wake or REM or light or deep. This explanation can be extended to other sleep states represented in other rows of Q matrix.

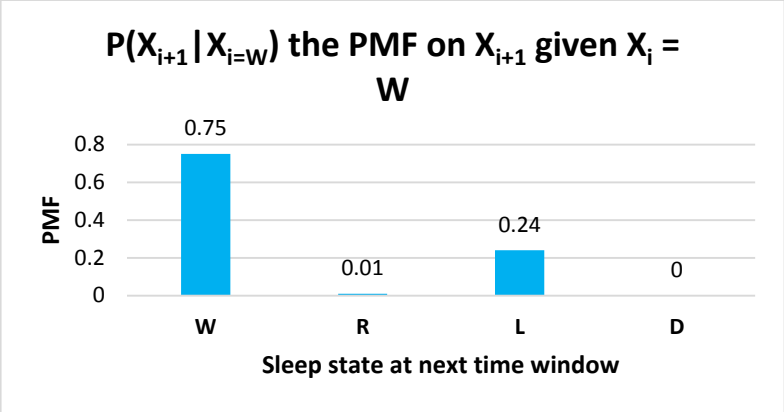

Figure 4.6: PMF values given that the current sleep state is wake (W)

It should be noticed that the given transition probability matrix is constrained based on well-studied sleep physiology of healthy subjects [4-8]. Transitioning from wake to deep, REM to deep and deep to REM sleep states is impossible, so these are assigned a probability value of 0.

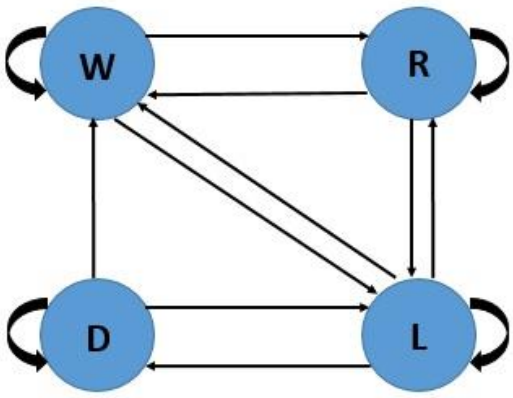

Figure 4.7: Sleep Stages – constrained state transition diagram for healthy subjects

The observed random variable Y corresponds to the log power feature extracted from the defined dominant frequency bands of EEG representative of different sleep states. Because EEG is a continuous time-series signal, the likelihood probability density R, where $R(b|a) = P(Y_i = b_i|X_i = a_i)$, in which given X, Y is modeled as a multi-variate Gaussian

whose conditional expectation is reflected in Table 4.1 and is defined by mean vector (μ) and covariance matrix (∑). R is the density of the Gaussian.

At time i, Y_i is a length-4 vector.

$$\mathbf{Y_i} = [\mathbf{Y_i^{\gamma}}\ \mathbf{Y_i^{\beta}}\ \mathbf{Y_i^{\sigma}}\ \mathbf{Y_i^{\delta}}]$$

Where Y_i corresponds to, for example Y = [1.61 1.18 -0.07 -2.44]

The likelihood matrix R is thus defined, for instance in the case when X = W as,

$$\mathbf{P(Y_i|X = W)} = \boldsymbol{\mathcal{N}}(\boldsymbol{\mu_W}, \boldsymbol{\Sigma_W}) \quad (6)$$

where $\mu_W = [\mu_W^{\gamma}\ \mu_W^{\beta}\ \mu_W^{\sigma}\ \mu_W^{\delta}]$ represents the mean vector given the sleep state is wake and Σ_W represents the covariance matrix. For instance, μ_W can take values [1.76 1.43 0.98 0.24].

To reiterate, Y is modeled as Gaussian represented by a mean μ and variance Σ.

If $b = [b^{\gamma}\ b^{\beta}\ b^{\sigma}\ b^{\delta}]$, then

$$\mathbf{f_{Y|X}(b|a)} = \frac{\mathbf{1}}{\sqrt{\mathbf{2\pi det\Sigma_a}}}\mathbf{e}^{(-\frac{\mathbf{1}}{\mathbf{2}}\mathbf{(b-\mu_a)^T\Sigma^{-1}(b-\mu_a)})} \quad (7)$$

Each element in the mean (μ) vector represents the probability density value of a particular frequency band given a particular sleep state.

Example, for wake stage – the mean vector (μ_W) looks like

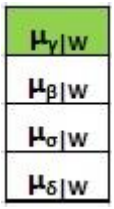

Figure 4.8: Representation of mean vector given sleep state = wake

For instance, the average log power in band γ during wake stage is represented by $\mu_{\gamma|W}$. And given a specific sleep state, a covariance matrix (Σ_a) describes how different frequency distributions co-vary with each other.

The typical values of the mean vector μ and covariance matrix ∑ have been chosen based on literature – backed evidence of the presence of dominant frequency bands in specific sleep stages given in the feature table 4.1.

	X = W	X = R	X = L	X = D	
μ =	0.2	0.1	0.1	-0.1	Y^{γ}
	-0.1	0.5	0.1	0.06	Y^{β}
	0.1	0.04	1.3	0.5	Y^{σ}
	-0.03	-0.3	0.1	0.7	Y^{δ}

Figure 4.9a: Each column represents typical mean (μ) vector values

	Y^{γ}	Y^{β}	Y^{σ}	Y^{δ}	
∑ =	0.7	0.1	0.3	-0.09	Y^{γ}
	0.01	0.8	0.4	0.1	Y^{β}
	0.4	0.3	1.2	1.5	Y^{σ}
	-0.1	0.1	0.4	9.8	Y^{δ}

Figure 4.9b: Typical covariance matrix (∑) values

This sums up the initialization of the HMM model parameters.

4.4 The Likelihood Function

Given the observation sequence $Y = \{Y_1 = b_1, Y_2 = b_2, \ldots, Y_T = b_T\}$ and a model $\theta = \{\pi, Q, R\}$, it is necessary to efficiently compute the likelihood function $P(Y; \theta)$ – the probability of the observation sequence given the model. The likelihood function, is the probability of recorded data as a function of unknown parameter.

In the case of HMM, this is obtained from the joint distribution by marginalizing over the hidden variables X = {$X_1 = a_1$, $X_2 = a_2$, …, $X_T = a_T$}

$$\mathbf{L}(\boldsymbol{\theta}) = \mathbf{P}(\mathbf{Y}|\boldsymbol{\theta}) = \sum_{\mathbf{X}} \mathbf{P}(\mathbf{Y}, \mathbf{X}|\boldsymbol{\theta}) \quad (8)$$

The likelihood function provides an objective means of assessing the "information" in a sample of data about the model parameter θ [4-9]. We would like to derive a summary that gives us a sense about the shape of the likelihood. This is provided by the maximum likelihood estimate.

4.4.1 Maximum Likelihood Estimation

For a fixed set of data and underlying statistical model, the method of maximum likelihood selects the set of values of the model parameters that maximizes the likelihood function. Intuitively, this maximizes the agreement of the selected model with the observed data [4-10]. For each sample point (b_1, b_2, …, b_n), let θ*(b_1, b_2, …, b_n) be a parameter value of which L(θ) attains a maximum as a function of θ for fixed (b_1, b_2, …, b_n).

θ*(b_1, b_2, …, b_n) is a maximum likelihood (ML) estimator (MLE) of the parameter θ [4-9]. In particular, if L(θ) is differentiable, we can consider

$$\frac{\partial \mathbf{L}(\boldsymbol{\theta})}{\partial \boldsymbol{\theta}} = \mathbf{0} \quad (9)$$

and check the conditions on

$$\frac{\partial^2 \mathbf{L}(\boldsymbol{\theta})}{\partial \boldsymbol{\theta}^2} \leq \mathbf{0} \quad (10)$$

to be sure that the estimate defines a maximum. This would mean that for a one-dimensional problem, verifying that the second derivative was negative. In likelihood

analyses, it is usually easier to work with log of the likelihood function, called the log-likelihood (log L(θ) , LL(θ)) instead of L(θ).

Hence, computing the MLE can often be formulated as finding θ* which solves the score equation:

$$\frac{\partial \mathbf{LL}(\boldsymbol{\theta})}{\partial \boldsymbol{\theta}} = \mathbf{0} \qquad (11)$$

From the total probability theorem, the log-likelihood function can be written as

$$\mathbf{LL}(\boldsymbol{\theta}) = \mathbf{log}\mathbf{L}(\mathbf{Y_1}, \dots, \mathbf{Y_T}; \boldsymbol{\theta}) = \mathbf{log}(\sum_{\mathbf{X_1}} \sum_{\mathbf{X_2}} \dots \sum_{\mathbf{X_T}} \mathbf{P}(\mathbf{X_1}, \dots, \mathbf{X_T}, \mathbf{Y_1}, \dots, \mathbf{Y_T}; \boldsymbol{\theta})) \qquad (12)$$

The method of maximum likelihood estimates θ, which is unknown and is referred to as the true value of the parameter, by finding a value of $\theta^* = \widehat{\boldsymbol{\theta}}_{\mathbf{MLE}}$ that maximizes LL(θ). This method of estimation defines a maximum likelihood estimator of θ, if any maximum exists

$$\widehat{\boldsymbol{\theta}}_{\mathbf{MLE}} = \underset{\boldsymbol{\theta}}{\mathbf{argmax}}\, \mathbf{LL}(\boldsymbol{\theta}) \qquad (13)$$

An MLE estimate is the same regardless of whether we maximize the likelihood or the log-likelihood function, since log is a monotonically increasing function.

Given that our objective is to find $\hat{\theta}_{\mathrm{MLE}}$ according to equation (13), the likelihood function parameterized by a nonrandom and unknown quantity θ, finding $\hat{\theta}$ directly from equation (12) is computationally intractable due to an exponential number terms to sum over [4-11]. Also, if the likelihood function has multiple local maxima, then any hill-climbing procedure can have problems with oscillating between multiple local maxima and never converge.

4.4.2 The Expectation – Maximization (EM) Algorithm

The expectation – maximization (EM) algorithm is an iterative method for finding maximum likelihood estimates of parameters in statistical models, where the model depends on unobserved latent variables.

The EM iteration alternates between performing an expectation (E) step, which creates a function for the expectation of the log-likelihood evaluated using the current estimate for the parameters, and a maximization (M) step, which computes parameters maximizing the expected log-likelihood found on the E step. These parameter-estimates are then used to determine the distribution of the latent variables in the next E step [4-12].

4.4.2.1 Reason for using EM algorithm for finding the parameters of HMM

If we have a HMM and we model $\theta = \{\pi, Q, R\}$. State space model for the latent process X is governed by –

$$\mathbf{P}(\mathbf{x_1}, \dots, \mathbf{x_T};\ \mathbf{Q}) = \boldsymbol{\pi}(\mathbf{x_1}) \prod_{\mathbf{i=2}}^{\mathbf{T}} \mathbf{Q}(\mathbf{x_i}|\mathbf{x_{i-1}}) \tag{14}$$

Q parameters pertaining to θ are related to the transition matrix values in the state-space model.

At each time i, Y_i is observed, which is a noisy version of X_i. The statistical model relating Y_i to X_i is termed the observation equation, of the form:

$$\mathbf{P}(\mathbf{y_i}|\mathbf{y_{i-1}}, \dots, \mathbf{y_1}, \mathbf{x_1}, \dots, \mathbf{x_T};\ \boldsymbol{\theta}) = \mathbf{R}(\mathbf{y_i}|\mathbf{x_i}) \tag{15}$$

If $y_1, \dots, y_T$ has been observed, then the joint distribution on the latent process and the observed process is given by

$$\mathbf{P}(\mathbf{x_1}, \dots, \mathbf{x_T}, \mathbf{y_1}, \dots, \mathbf{y_T}; \boldsymbol{\theta}) = \mathbf{P}(\mathbf{x_1}, \dots, \mathbf{x_T}; \boldsymbol{\theta})\mathbf{P}(\mathbf{y_1}, \dots, \mathbf{y_T}|\mathbf{x_1}, \dots, \mathbf{x_T};\ \boldsymbol{\theta})$$

$$\Rightarrow \mathbf{P}(\mathbf{x_1}, \dots, \mathbf{x_T}, \mathbf{y_1}, \dots, \mathbf{y_T}; \boldsymbol{\theta}) = \boldsymbol{\pi}(\mathbf{x_1}) \prod_{\mathbf{i=2}}^{\mathbf{n}} \mathbf{Q}(\mathbf{x_i}|\mathbf{x_{i-1}})\mathbf{R}(\mathbf{y_i}|\mathbf{x_i}) \quad (16)$$

Denoting the joint distribution as $P(y_1, \dots y_T; \theta)$ where $\theta = \{\pi, Q, R\}$ and considering the set of values that can be taken by X = {W, R, L, D} (n = 4), attempting to do brute – force maximum-likelihood estimation by maximizing the log-likelihood with respect to θ is easily seen to become a very complicated calculation with no analytical result as shown in the equations below. (eq. 17 from [4-11])

$$\mathbf{log}\, \mathbf{P}(\mathbf{y_1}, \dots \mathbf{y_T};\ \boldsymbol{\theta}) = \mathbf{log}(\textstyle\sum_{\mathbf{x_1=1}}^{\mathbf{n}} \dots \sum_{\mathbf{x_T=1}}^{\mathbf{n}} \boldsymbol{\pi}(\mathbf{x_1}) \prod_{\mathbf{i=2}}^{\mathbf{T}} \mathbf{Q}(\mathbf{x_i}|\mathbf{x_{i-1}})\, \mathbf{R}(\mathbf{y_i}|\mathbf{x_i})) \quad (17)$$

$$\mathbf{log}\, \mathbf{P}(\mathbf{y_1}, \dots \mathbf{y_T};\ \boldsymbol{\theta}) = \mathbf{log}(\textstyle\sum_{\mathbf{x_1=1}}^{\mathbf{n}} \dots \sum_{\mathbf{x_T=1}}^{\mathbf{n}} \mathbf{P}(\mathbf{x_1}, \dots, \mathbf{x_T}, \mathbf{y_1}, \dots, \mathbf{y_T};\ \boldsymbol{\theta})) \quad (18)$$

This is why the EM algorithm is seen to useful. EM algorithm has the following favorable properties:

- It always converges to a local maximum of the likelihood function
- If the likelihood function has only one local maximum (which is also the global maximum), it will always converge to it.

Determining a method to adjust the model parameters, $\theta = \{\pi, Q, R\}$, to maximize the probability of the observation sequence given the model, $P(Y;\theta)$ is the most difficult problem of HMMs [4-13]. For any finite observation sequence as training data (which in our case, is the power feature extracted from EEG signal acquired using epidermal or conventional electrode), we can choose $\theta = \{\pi, Q, R\}$ such that $P(Y;\theta)$ is locally maximized as a function of theta using an iterative procedure such as the Baum – Welch algorithm (which is just a special case of EM algorithm) [4-14].

Given the hidden variable $X = (X_1 = a_1, \dots, X_T = a_T)$ and the observed variable $Y = (Y_1 = b_1, \dots, Y_T = b_T)$, we can define $\widetilde{P}$ as the probability of being in state a_i at time i and

state a_{i+1} at time (i+1), given the model (θ) and observation sequence (Y). $\widetilde{P}$ can be mathematically represented as

$$\widetilde{\mathbf{P}} = \mathbf{P}(\mathbf{X_i} = \mathbf{a_i}, \mathbf{X_{i+1}} = \mathbf{a_{i+1}} | \mathbf{Y_{1:T}}, \boldsymbol{\theta}) \tag{19}$$

Maximizing the likelihood function can be expressed as

$$\max_{\boldsymbol{\theta}} \mathbf{L}(\boldsymbol{\theta}) = \max_{\widetilde{\mathbf{P}}} \max_{\boldsymbol{\theta}} \mathbf{J}(\boldsymbol{\theta}, \widetilde{\mathbf{P}}) \tag{20}$$

This leads us into the iterative procedure of maximizing $\widetilde{P}$ as part of the expectation step (E – step) and maximizing θ as part of the maximization step (M – step).

E – Step: is the process of calculating the posterior on x given y. It is nothing more than finding a conditional distribution, as defined by equation (20). Since $Y = (Y_1, \ldots, Y_T)$ is fixed, we use the law of conditional probability to calculate the $\widetilde{P}$ matrix containing 4^T entries (corresponding to n = 4 discrete latent states) for the M-step.

Using equation (20), by virtue of Baum – Welch algorithm, we can efficiently calculate the conditional probabilities:

$$\widetilde{P}(X_1, X_2) = P(X_1, X_2 | Y_1, \ldots, Y_T;\ \theta) \text{ (containing 16 entries)}$$

$$\widetilde{P}(X_2, X_3) = P(X_2, X_3 | Y_1, \ldots, Y_T;\ \theta) \text{ (containing 16 entries)}$$

$$\widetilde{P}(X_{T-1}, X_T) = P(X_{T-1}, X_T | Y_1, \ldots, Y_T;\ \theta) \text{ (containing 16 entries)}$$

This gives a total of 16T entries instead of 4^T entries. Only 16T entries are required to implement the EM algorithm.

The **M – step** uses the hidden variables estimated in the previous E – step to identify the optimum θ values corresponding to the estimated hidden states.

The E – step can be summarized as

$$\widetilde{\mathbf{P}}[\mathbf{k}] = \underset{\widetilde{\mathbf{P}}}{\mathbf{argmax}}\, \mathbf{J}(\widehat{\boldsymbol{\theta}}\,[\mathbf{k}-\mathbf{1}], \widetilde{\mathbf{P}}) \tag{21}$$

and the M – step can be represented as

$$\widehat{\boldsymbol{\theta}}[\mathbf{k}] = \underset{\boldsymbol{\theta}}{\mathbf{argmax}}\, \mathbf{J}(\boldsymbol{\theta}, \widetilde{\mathbf{P}}[\mathbf{k}]) \tag{22}$$

This end result of EM algorithm gives rise to an optimum set of values $\widetilde{P}^*$ and θ^*

Expectation Step (E-Step)
Use current parameters $\theta = \{\pi, Q, R\}$ and observations $(Y_{1:T})$ to reconstruct the hidden structure $(X_{1:T})$.

Maximization Step (M-Step)
Use the hidden structure and the observations to reestimate the parameters $\theta^* = \{\bar{\pi}, \bar{Q}, \bar{R}\}$.

(Repeat until convergence when the ML parameters are found)

The EM algorithm always converges to a fixed point and that fixed point is a local maximum to the likelihood function. The convergence condition is given as –

$$\|\boldsymbol{\theta}[\mathbf{k}] - \boldsymbol{\theta}[\mathbf{k}-\mathbf{1}]\| < \varepsilon \tag{23}$$

Where ε is assigned a small tolerance value. Pictorially, the EM algorithm can be depicted as shown in Figure 4.10.

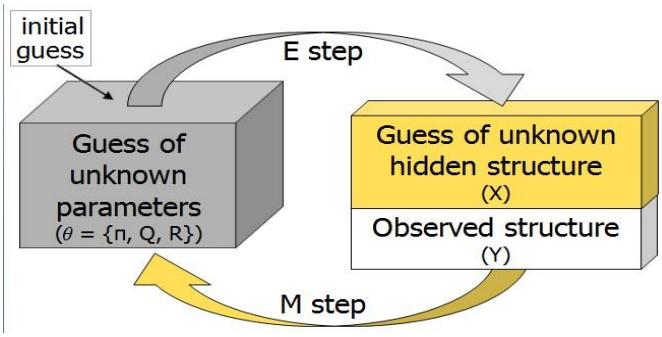

Figure 4.10: EM algorithm

where initial guess = initial guess on the parameters of the model ($\theta = \{\pi, Q, R\}$)

The ML estimate of the parameters obtained using the EM algorithm are consistent with what makes physiological sense according to feature Table 4.1 and Q matrix as shown in figure 4.5.

In case of our sleep study paradigm, once the EM algorithm converges to the reestimated parameter values $\{\hat{\pi}, \hat{Q}, \hat{R}\}$ from the observed EEG signal data, we use another mathematical technique called the Maximum a Posteriori (MAP) sequence estimation to identify the hidden sleep staging.

4.5 Maximum a Posteriori sequence estimation

Given the observation sequence $Y = Y_1,\ldots,Y_T$ and the model θ, the question arises as to how to identify one corresponding state sequence $X = X_1, \ldots, X_T$ that is the best explanation of the observations. This is addressed by the technique of Maximum a Posteriori (MAP) sequence estimation.

The MAP procedure obtains a point estimate (single value that serves as the "best guess/ estimate") of an unobserved quantity on the basis of empirical data. Given the data, the MAP procedure employs an optimization that incorporates a prior belief over the quantity one wants to estimate. Given the entire set of observation values $Y_{1:T} = b_{1:T}$, the MAP rule that gives the best sequence estimate of the hidden random process X^n is mathematically represented as:

$$\hat{\mathbf{x}}_{\mathbf{MAP}}^{\mathbf{T}} = \underset{\mathbf{a_1}\epsilon\{\mathbf{1},\ldots,\mathbf{n}\},\ldots,\mathbf{a_T}\epsilon\{\mathbf{1},\ldots,\mathbf{n}\}}{\mathbf{argmax}} \mathbf{P}(\mathbf{X_{1:T}} = \mathbf{a_{1:T}} | \mathbf{Y_{1:T}} = \mathbf{b_{1:T}};\ \boldsymbol{\theta}) \quad (24)$$

Where at every time point, $X_i = a_i$ can take values from 1:n possible states and T indicates the total number of time points. Here θ represents the result of EM algorithm,

$\hat{\theta}_{\mathrm{MLE}}$. For a large n, finding the most likely path involves n^T different possible sequences to search over to perform the maximization. This is computationally infeasible [4.15].

4.5.1 The Viterbi Algorithm

The MAP sequence estimate is implemented using a computationally efficient Viterbi algorithm. This algorithm helps in finding the most likely sequence of hidden states (Viterbi Path) – by interpreting the shortest path from source to destination (first time point to the last or T^{th} time point). It utilizes the principle of backward induction (also termed dynamic programming) for the purpose of finding the most likely sequence efficiently. The path begins with state value a_{i-1} at time i-1 and ends at state φ at time T+1. The shortest path from a_i to φ is determined based on the 'cost-to-go' function (denoted by J) which is defined for every possible state transition from one time point to the next.

Assuming the time axis is from {0, …, T+1} rather than being {1, …, T} and hardwiring $a_0 = \phi$ and $a_{T+1} = \phi$, we represent the distance between state at time i and state at time i+1 as $d_i(a_{i-1}, a_i)$. MAP sequence estimate as computed using the Viterbi algorithm is given by:

$$\hat{\mathbf{x}}_{\mathbf{MAP}}^{\mathbf{T}} = \underset{\mathbf{x}}{\mathbf{argmax}}\, \mathbf{P}(\mathbf{x}|\mathbf{y}) = \underset{\mathbf{x}}{\mathbf{argmin}} -\mathbf{log}\, \mathbf{P}(\mathbf{x}|\mathbf{y}) \tag{25a}$$

$$\text{where } \mathbf{d_i}(\mathbf{a_{i-1}}, \mathbf{a_i}) = -\mathbf{log}[\mathbf{Q}(\mathbf{x_i}|\mathbf{x_{i-1}})\, \mathbf{R}(\mathbf{y_i}|\mathbf{x_i})] \tag{25b}$$

$$\hat{\mathbf{x}}_{\mathbf{MAP}}^{\mathbf{T}} = \underset{\mathbf{a_1}\epsilon\,\{1,\ldots,n\},\ldots,\mathbf{a_T}\{1,\ldots,n\}}{\mathbf{argmin}} \sum_{\mathbf{i=1}}^{\mathbf{T+1}} \mathbf{d_i}(\mathbf{a_{i-1}}, \mathbf{a_i}) \tag{26}$$

Intuitively, this can be explained using an analogy that if the shortest path from Chicago to Los Angeles goes through Minneapolis, then the shortest path from

Minneapolis to Los Angeles must be along the same shortest path. Formally, considering the optimal MAP estimate $\hat{x}_{MAP}^{T} = (a_1^*, \dots, a_T^*)$, for every i for which $1 \le i \le T$:

$$\sum_{j=i}^{T+1} \mathbf{d_j}\left(\mathbf{a_{j-1}^*}, \mathbf{a_j^*}\right) \le \sum_{j=i}^{T+1} \mathbf{d_j}(\mathbf{a_{j-1}}, \mathbf{a_j}) \quad (27)$$

For all $(a_i, a_{i+1}, \dots a_T, a_{T+1})$ for which $a_i = a_i^*$ and $a_{T+1} = \phi$

The model parameters that are used for computing the distance metric are obtained using EM algorithm.

Inner Workings of Viterbi

The computation process moves backwards in time – beginning at the $(T+1)^{th}$ time point with the cost function to go to all the states at the T^{th} time point assumed to be 0. The minimum distance (d) to transition from each state of the T^{th} time point to every possible state of the $(T-1)^{th}$ time point is calculated based on Q and R matrix values. The minimum cost function for transitioning from each state is based on the minimum distance value summed with the cost function for the previous transition. The optimal decision of cost and state value are stored. The iterative process is repeated until the first time point. In our case, distances are logs of probabilities. Based on the minimum cost function, the shortest path is traced. Hence the optimal sequence satisfying $\hat{x}_{MAP}^{T} = \{a_1^*, a_2^*, \dots, a_T^*\}$ is obtained.

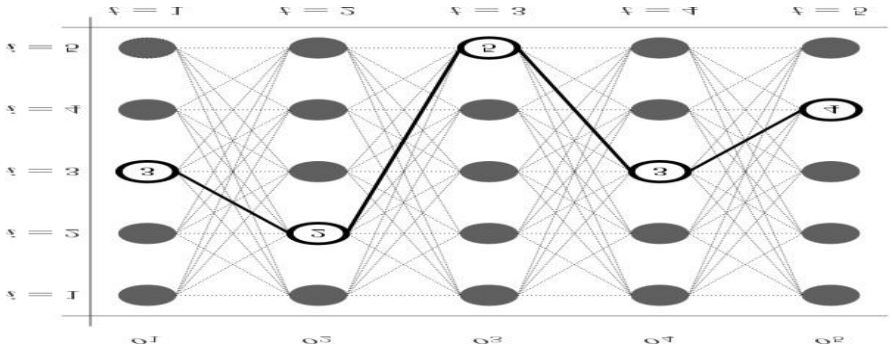

Figure 4.11: Most likely sequence estimation using Viterbi Algorithm (Source: Wikimedia Commons)

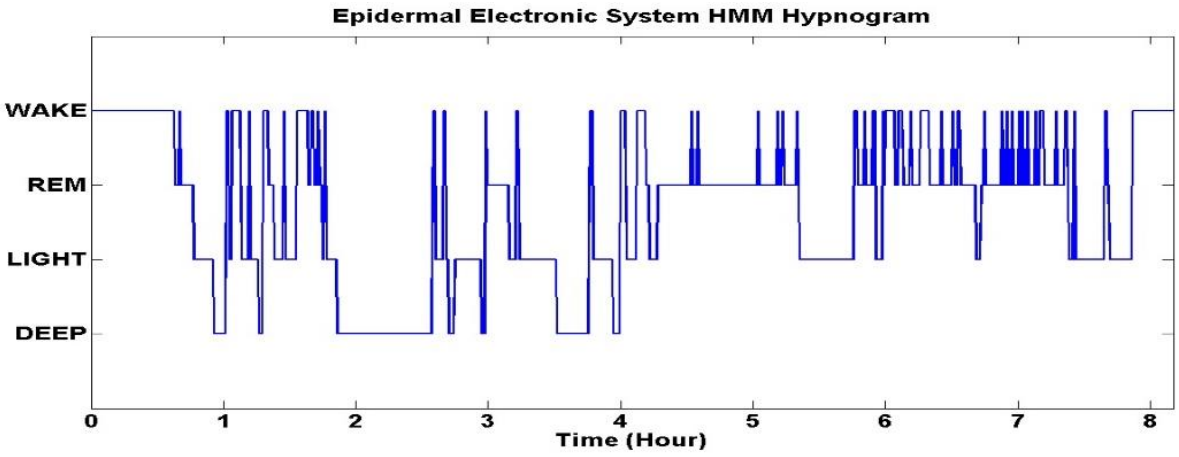

Figure 4.12: Hypnogram plot built for one subject

4.6 Comparison of two electrode technologies

In this pilot study, the ultimate goal is to compare the efficacy of a novel epidermal electronic sensor against already established conventional electrodes for the purpose of sleep monitoring. Given this aim, the comparison can be performed at three levels – input to the HMM (power features), parameter space (π, Q, R) and output sleep staging. This framework is shown in figure [4-13]. In this thesis, we compare the two systems at the input level, by performing a hypothesis test on the input power features of the two technologies.

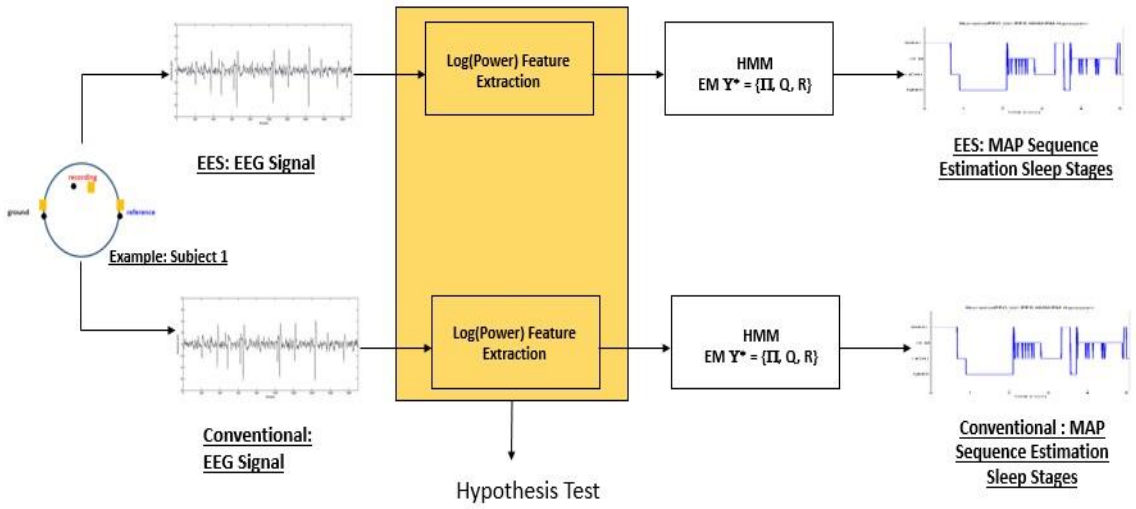

Figure 4.13: Framework for comparison of two electrode technologies

4.6.1 A note on hypothesis testing

In hypothesis testing, we have two different explanations of data. One explanation, the null hypothesis (H_0), corresponds to a class of statistical models that pertain to "happening by chance". The other explanation, the alternate hypothesis (H_1), corresponds to a different class of statistical models that pertain to some hypothesized structure in the statistical properties of the data [4-16]. For instance, in our case, we want to compare two different explanations of our EEG and epidermal data. One explanation is that the simultaneous recording are statistically independent and came from chance. The other hypothesis is that they both reflect an underlying "true EEG signal" plus noise. When we perform hypothesis testing, we observe data and first take some pre-processing of the data, by forming a "test statistic" (*for example, in our case, a covariance/mean-squared-error/correlation-coefficient between epidermal and conventional EEG*). With this test statistic, we attempt to understand how likely we could have observed this from one hypothesis or another. In general, we form the test statistic so that it is on one extreme

under the null hypothesis (e.g. small) and on the other extreme under the alternate hypothesis (e.g. large). Typically, we are attempting to test a hypothesis that the data is explained by the alternate hypothesis but we must first be skeptics. Specifically, before we can declare that our findings are statistically significant, we have to first make sure that the probability that it – or something more extreme - skeptically happened by chance is sufficiently small. A p-value gives us exactly that calculation: the probability, under the null hypothesis, that the test statistic would have been what we observed or something more extreme. If the p-value is sufficiently small (e.g. below 0.05), then we "reject" the null hypothesis and can confidently declare that what we have observed is indeed statistically significant. If, on the flipside, the p-value is not sufficiently small, then we fail to reject the null hypothesis.

4.6.2 Nonparametric hypothesis test

In general, to calculate a p-value, we have to know the probability distribution of the test statistic under the null hypothesis. In many situations with non-stationary physiological data (such as EEG), we do not a priori have a model for what this probability distribution is. Nonparametric tests are performed when certain assumptions cannot be made about the data that they are drawn from a specific probability distribution [4-17]. These are based upon empirical distribution and the underlying model can grow in size according to the complexity of the data, hence these are said to be more robust than parametric hypothesis tests.

In our setting, we assume that the conventional electrode is recording "signal + noise". We have different hypothesis about the epidermal electrodes, H_0 being that they

just record noise and H_1 being that they record signal + noise. So in summary, we have the following models for our hypothesis test:

- H_0: Under the null hypothesis, conventional electrode records 'EEG signal + noise' whereas epidermal electrode records only 'noise'
- H_1: Under the alternate hypothesis, we propose that both conventional and epidermal electrodes record 'EEG signal + noise'

We make the observation that under the null hypothesis, the epidermal electrode signals are statistically independent of conventional recordings. On the flipside, under the alternate hypothesis, because they both contain a "signal + noise", they will not be statistically independent. We used this observation to guide our selection of 3 test statistics, all of which have extreme values on the independent side, as compared to the dependent side. Each test statistic takes as input EEG wave forms from a conventional electrode as well as an epidermal electrode and is given as follows:

A. Mean squared error between epidermal and conventional waveforms

B. Covariance between epidermal and conventional waveforms

C. Correlation coefficient between epidermal and conventional waveforms

Note that for test statistic A: it should be large under H0 and small under H1. For test statistics B and C: they should be small under H0 and large under H1.

4.6.2.1 Methodology (Bootstrapping)

Bootstrapping is employed as the method to contruct the hypothesis test. Since boostrapping technique is distribution – independent, it provides a convenient, indirect method to assess the properties of the distribution underlying the sample [4-18]. The usage

of this technique is justified based on the experiement we performed in which our observations, namely, the EEG signals are independent and identically distributed (i.i.d.) for every subject in the population. The idea behind bootstrapping is that the inference about a population from sample data can be modeled by resampling the sample data and performing inference on [4-19]. It works by treating the inference of true probability distribution J, given the original data, as being analogous to inference of empirical distribution of $\hat{J}$, given the resampled data. Since $\hat{J}$ is known, the accuracy of inferences regarding $\hat{J}$ from the resampled data can be assessed. If $\hat{J}$ is a reasonable approximation of J, then the quality of inference on J can in turn be inferred.

In the case of our data, we have 10 simultaneously recorded sleep EEG signals from epidermal and conventional electrodes, giving rise to a total of 10 actual pairs of data. The bootstrapped pairs of data are obtained by combining epidermal electrode data of one subject with conventional electrode data of another subject. Note that when calculating test statistics in this manner, because they are different subjects, and thus the conventional waveform is statistically independent of the epidermal one, this is a sample from the null hypothesis. Because we have 10 subjects, this allows for 10*(10-1)=90 different pairs pertaining to independent samples of the test statistic under H0. Note that the bootstrapped data correspond to the test statistics calculated using the non-actual pairs of data, as shown in the yellow matrix elements in the figure below.

Using the bootstrapped samples, we construct a histogram of the bootstrapped test statistics, contributing to the distribution under the null hypothesis H_0.

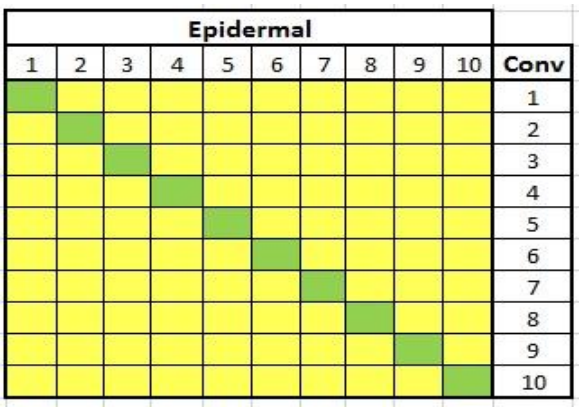

Figure 4.14: Illustration of what the bootstrapped data constitutes (yellow boxes)

The value of the test statistic as calculated using the original pair of EEG, for instance, subject 1 epidermal vs. conventional is plotted alongside the bootstrapped histogram. A one-tailed statistical significance test is performed to calculate the p-value of the chosen test statistic and make inferences based on the result of the calculation. The distribution for the hypothesis test is obtained by performing bootstrapping under the null hypothesis (H_0).

Recalling that the power of EEG contains T time windows (for every 30 s epoch), we consider frequency bins (f = 709) corresponding to the bands of frequencies of interest in our sleep study paradigm, which is 0-50 Hz. The power matrix used for comparison is of f X T dimension.

Y_{EPI} and Y_{CONV} are the EEG power matrices of f X T dimension.

At time window t,

$$\mathbf{Y_{EPI}(t)} = \boldsymbol{\mu}_{\mathbf{t}}^{\mathbf{EPI}} + \boldsymbol{\varepsilon}_{\mathbf{t}} \quad \text{(Under H1)} \qquad (28)$$

Where μ_t^{EPI} represents the power signal across 0-50 Hz at time window t, for epidermal electrodes and ε_t represents Gaussian noise such that $\varepsilon_t \sim \mathcal{N}(0, \sigma_\varepsilon^2)$

Similarly for conventional electrodes,

$$\mathbf{Y_{CONV}(t)} = \mathbf{\mu_t^{CONV}} + \mathbf{e_t} \text{ (Under H1)} \quad (29)$$

e_t represents Gaussian noise such that $e_t \sim \mathcal{N}(0, \sigma_e^2)$

4.6.2.2 Rationale behind the choice of test statistics

Mean squared error (MSE) of an estimator measures the average of the square of errors, that is the difference between the estimator and what is estimated [4-20]. It is a risk function that corresponds to the expected value of the squared error loss.

If $\hat{Y}$ is a vector of n predictions, and Y is a vector of true values then MSE is mathematically represented as

$$\mathbf{MSE} = \frac{\mathbf{1}}{\mathbf{n}} \sum_{\mathbf{i=1}}^{\mathbf{n}} (\widehat{\mathbf{Y}}_\mathbf{i} - \mathbf{Y_i})^\mathbf{2} \quad (30)$$

In the case of our hypothesis test, the squared error (SE) distance (d(t)) between the power feature values of epidermal (equivalent to the predicted value) and conventional (equivalent to the true value) is given as

$$\mathbf{SE} = \mathbf{D(t)} = \|\mathbf{Y_{EPI}}(:, \mathbf{t}) - \mathbf{Y_{CONV}}(:, \mathbf{t})\|^\mathbf{2} \quad (31)$$

Where t represents each time window

D(t) is a vector of [1 X T] dimension

The MSE across all time windows is $MSE\ (SE) \stackrel{\text{def}}{=} TS(Y_{EPI}, Y_{CONV})$

$$\mathbf{TS_a}(\mathbf{Y_{EPI}} - \mathbf{Y_{CONV}}) = \frac{\mathbf{1}}{\sqrt{\mathbf{T}}} \sum_{\mathbf{t=1}}^{\mathbf{T}} \mathbf{SE(t)} \quad (32)$$

The estimator of MSE in our case is the power feature.

Intuitively, if MSE is zero, the estimator (Y_{EPI}) predicts the observations of parameter (Y_{CONV}) with prefect accuracy. In reality, MSE should be close to zero if the two

EEG signals being compared are similar and the measurement noise is small. The actual epidermal vs. conventional EEG signal is compared against the bootstrapped distribution.

Covariance is a measure of how much two random variables vary with respect to each other [4-21]. The covariance is positive, if greater or smaller values of one variable correspond to the respective greater and smaller values of another variable. Conversely, if the variables show opposite behavior, then the covariance is said to be negative. If the covariance is zero, then the random variables are uncorrelated.

Mathematically, the covariance between two jointly distributed real-valued random variables x and y is defined as –

$$\boldsymbol{\sigma(x,y) = E[(x - \mu_x)(y - \mu_y)]} \qquad (33)$$

Where the expected value (mean) of the random variable can be written as $\mu_x = E[x]$ and $\mu_y = E[y]$

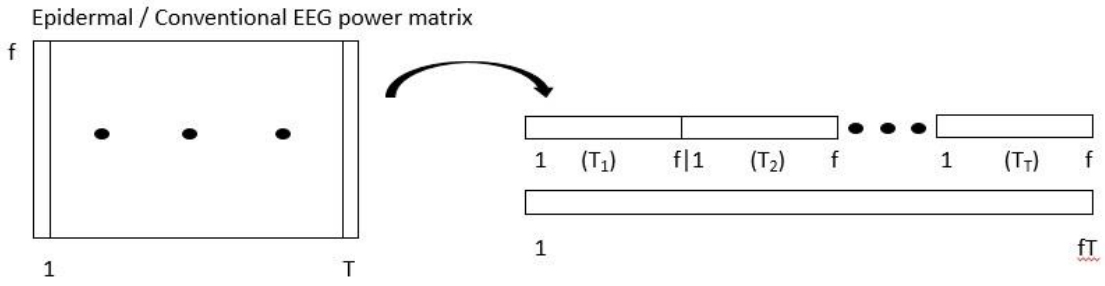

Figure 4.15: Building power vector to calculate the covariance

Considering covariance as a test statistic to estimate if epidermal and conventional electrodes record similar EEG signal, hypothesis test is performed on the power feature. Using similar rationale as in the case of MSE, we can represent covariance as

$$\mathbf{TS_b(Y_{EPI}, Y_{CONV}) = \frac{1}{\sqrt{fT}} \sum_{t=1}^{fT}[(Y_{EPI}^{f,T} - \mu_{EPI})(Y_{CONV}^{f,T} - \mu_{CONV})]} \qquad (34)$$

The normalized version of covariance is **correlation coefficient** [4-22]. It is a measure of linear correlation dependence between two random variables X and Y giving a value included and between +1 and -1; where 1 is total positive correlation, -1 is total negative correlation and 0 is no correlation. It is defined as the covariance of two variables divided by the product of their standard deviations. Mathematically, correlation coefficient $\rho_{X,Y}$ is given as

$$\boldsymbol{\rho_{X,Y}} = \frac{\mathbf{cov(X,Y)}}{\boldsymbol{\sigma_X \sigma_Y}} \tag{35}$$

Considering correlation coefficient as another test statistic,

$$\mathbf{TS_c(Y_{EPI}, Y_{CONV})} = \frac{\mathbf{TS_b}}{\boldsymbol{\sigma_{EPI}\sigma_{CONV}}} \tag{36}$$

The results of comparison are shown in the next chapter.

Chapter 5 – Results

In this chapter, we give an overview of the subject descriptors, preprocessing results, time – frequency plots and results of the hypothesis tests.

5.1 Subject descriptors

Based on the inclusion criteria given in section 3.1, 14 subjects were recruited. The table below shows the descriptive details of each subject.

Table 5.1: Subject descriptors

Subject #	Age	Gender	Medical Problems	Sleep deprived	Completed study	Hours captured	Data Included in the study?
1	35	M	No	No	Yes	~8	Yes
2	22	F	No	No	Yes	~5.5	Yes
3	20	F	No	No	Yes	~8	Yes
4	28	M	No	No	Yes	~8	Yes
5	25	M	No	No	Yes	~8.5	Yes
6	35	M	No	No	Yes	~7	Yes
7	25	F	No	No	Yes	~8	Yes
8	34	M	No	No	Yes	~8	Yes
9	23	M	No	No	Yes	~7	Yes
10	21	M	No	No	Yes	~7	Yes
11	26	M	No	No	Yes	~8	No
12	23	F	No	No	Yes	~8	No
13	21	M	No	No	Yes	~8	No
14	23	M	No	No	Yes	~8	No

Although the last four subjects completed the sleep recording, they weren't included in the pool of data used to perform hypothesis tests on to arrive at an inference because of the following reasons:

- Subjects 11, 12 – skin impedance was very high and the signal was completely saturated
- Subjects 13, 14 – one of the avatar amps had issues only in these two recordings with signal sampling and storage
- Subject 11, 13, 14 – shelf life of the first electrode (GS26, section 2.x) was exceeded resulting in signal saturation

5.2 Raw EEG Plot

The raw EEG data from epidermal and conventional electrodes are plotted simultaneously for comparison. It can be noticed from figure [5.1] that the raw EEG signal from epidermal electrode is prone to more drift in comparison with its counterpart from the conventional electrode.

The two EEG signals are high – pass filtered using least – square linear phase FIR filter of cut-off 0.5 Hz. Shown below is an example of filtered and unfiltered versions of simultaneously recorded signal from a subject.

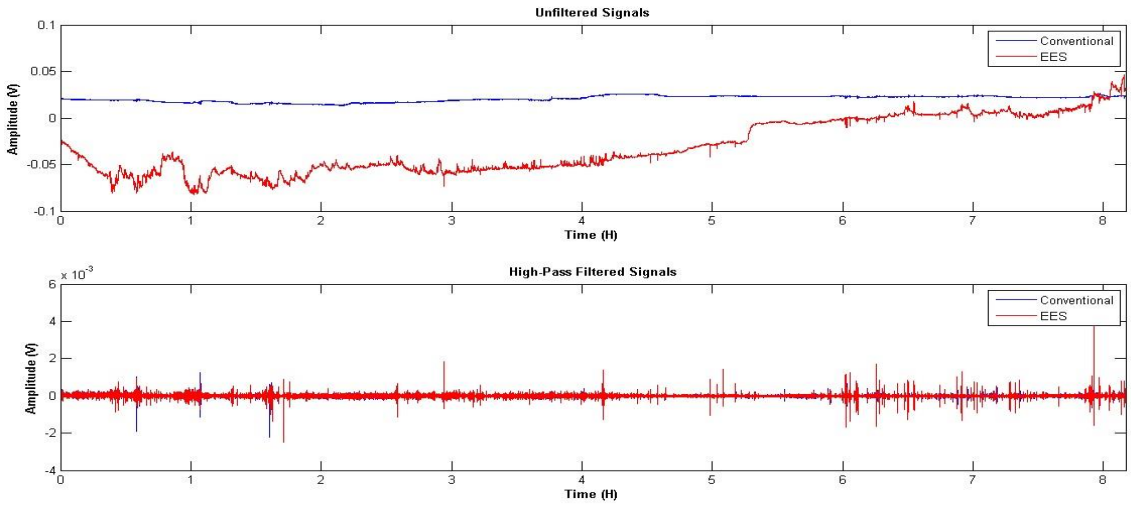

Figure 5.1: Unfiltered vs. Filtered Signals

5.3 Time – frequency spectrogram

The raw signals are processed and EEG power is extracted, time – frequency spectrogram is plotted. Reproducing one part of the figure from section 4, figure 4.1.

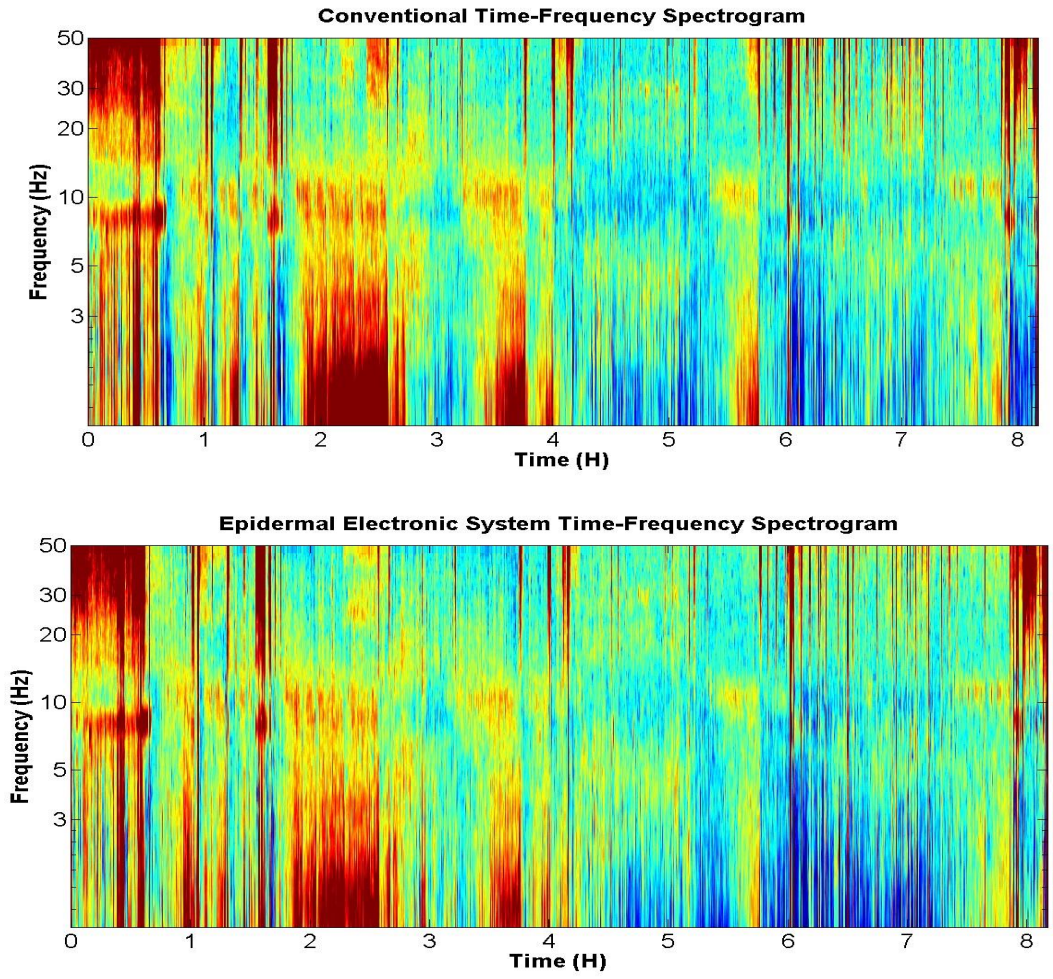

Figure 5.2: Time-frequency spectrogram plots of conventional and epidermal electrodes for one subject. Qualitatively, they are similar.

5.4 Hypnogram

Based on the mathematical framework we have defined, hypnograms are generated

for each subject. One example figure of the hypnogram, repeated from Figure 4.12 is here. For this subject, the hypnograms built for sleep EEG signals acquired using the two electrodes are similar.

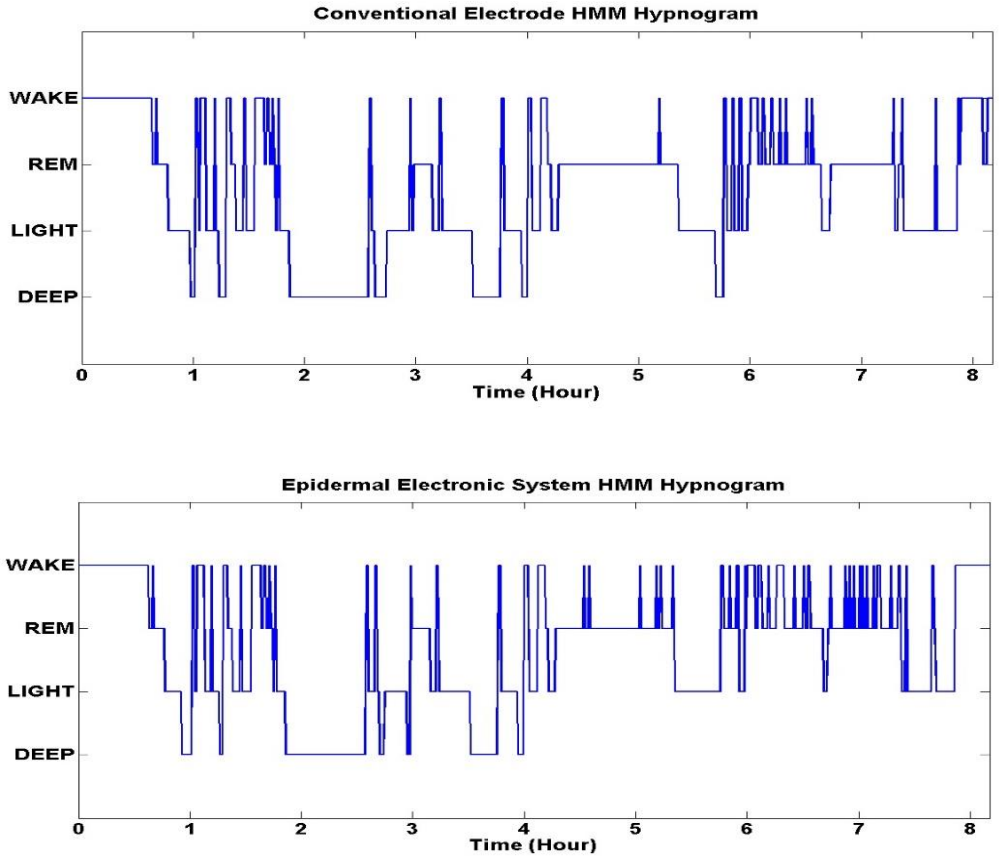

Figure 5.3: Hypnogram plots of one subject

5.5 Results of hypothesis tests

Recalling the hypothesis test,

H_0: Under the null hypothesis, conventional electrode records 'EEG signal + noise' whereas epidermal electrode records only 'noise'

H_1: Under the alternate hypothesis, we propose that both conventional and epidermal electrodes record 'EEG signal + noise'

The figures below show each of the three classes of test statistics (red lines), along with the bootstrapped test statistic distribution under the H_0.

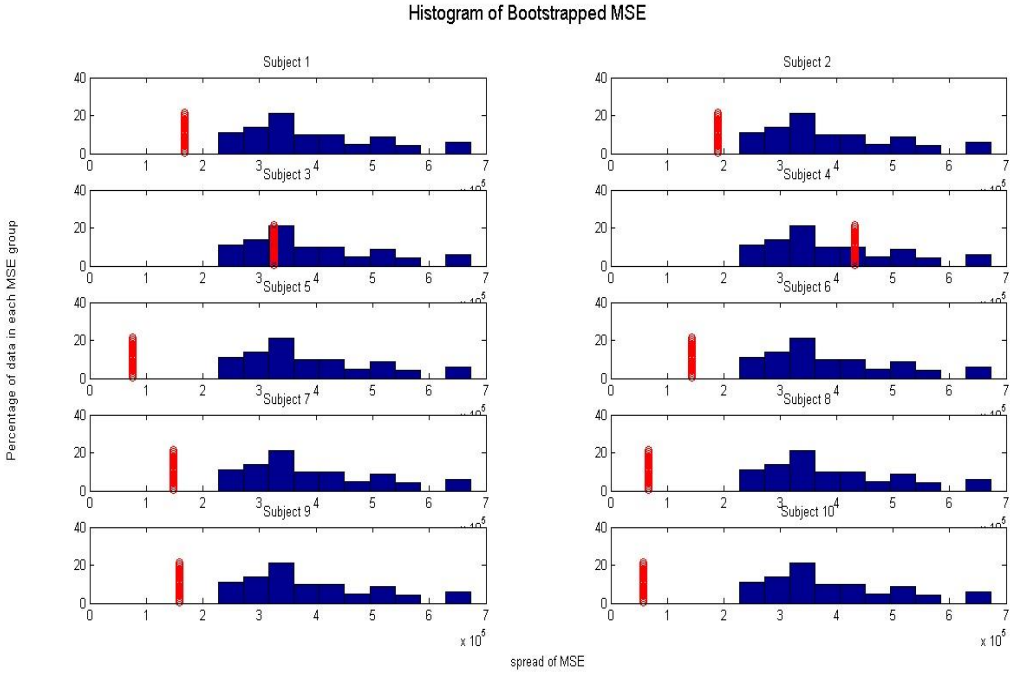

Figure 5.4a: Histogram of bootstrapped mean squared error (MSE)

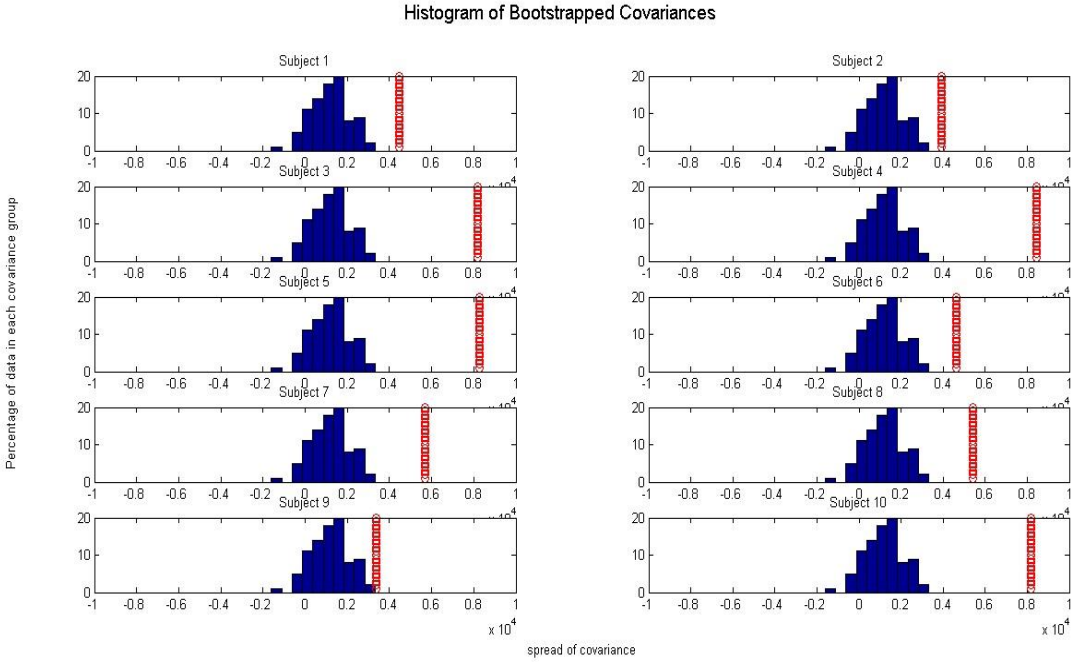

Figure 5.4b: Histogram of bootstrapped covariance

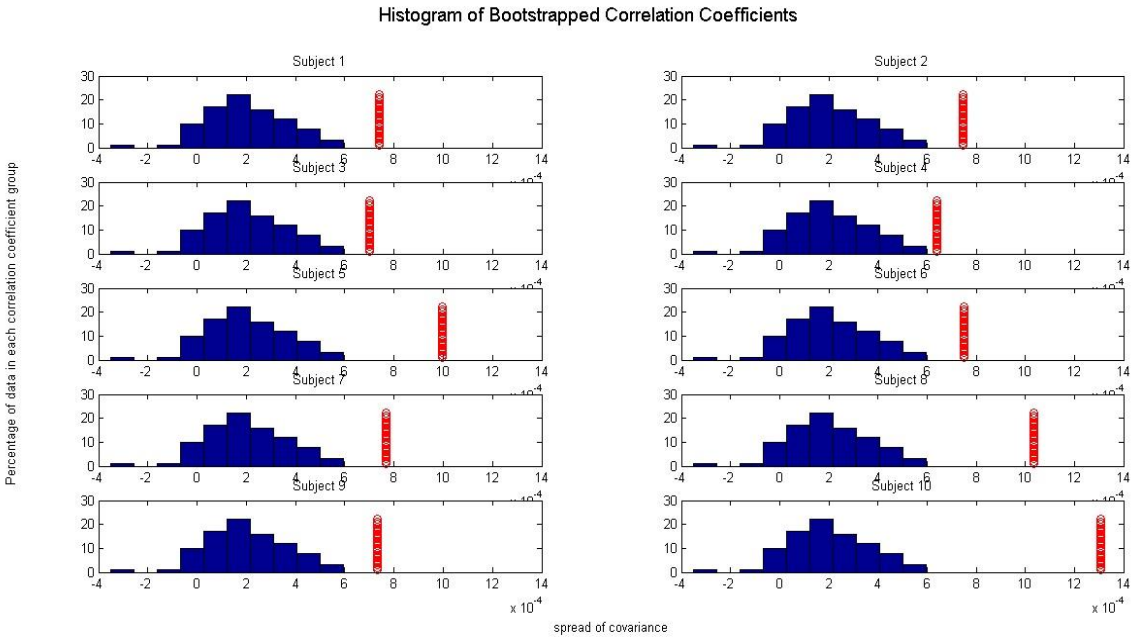

Figure 5.4c: Histogram of correlation coefficient

Table 5.2: P-values of the chosen 3 test statistics

Subject #	P-value of MSE	P-value of Covariance	P-value of Correlation Coefficient
1	0.010989011	0.010989011	0.010989011
2	0.010989011	0.010989011	0.010989011
3	0.351648352	0.010989011	0.010989011
4	0.659340659	0.010989011	0.010989011
5	0.010989011	0.010989011	0.010989011
6	0.010989011	0.010989011	0.010989011
7	0.010989011	0.010989011	0.010989011
8	0.010989011	0.010989011	0.010989011
9	0.010989011	0.010989011	0.010989011
10	0.010989011	0.010989011	0.010989011

Test statistic A

The MSE values of subject 3 and 4 are in a range comparable to that of the bootstrapped MSE values. Hence, their p-values are large. This could also probably be

because the statistical power values of the number of subjects that the study has been performed on and the bootstrapped samples are very less.

For the other subjects, the p-value = 0.01. Based on this value, H_0 can be rejected for 8 subjects. In these cases, the alternate hypothesis that both epidermal and conventional electrodes record EEG signal + noise is more plausible.

Test statistic B

For covariance, based on the p-value = 0.01 H_0 can be rejected and H_1 can be stated to be the more plausible alternative. Epidermal and conventional electrode EEG signals co-vary well with each other.

Test statistic C

P-value = 0.01 for all subjects. H_0 can be rejected. Correlation coefficients of epidermal and conventional signals are positive.

Based on these experimental results, it can be seen that epidermal electrodes have the capability to function as effectively as conventional electrodes.

Chapter 6 – Discussion

In this chapter, we give an overview of the possible sources of error, future directions and potential impact of this research.

6.1 Sources of error

Based on the problems encountered while conducting the experiment, the following observations have to be carefully considered for future studies. Skin preparation is highly crucial for long – term recording EEG signal during sleep. Abrading the skin with 3M red dot trace prep was found to be very effective in most of the subjects. However, because some subjects had given us a subjective statement that they were allergic to skin abrasion, effective skin prep was not always possible. This led to a high skin impedance and signal saturation shortly after the recording began. This is the reason why the recordings of subject 11 and 12 could not be included in the simultaneous study.

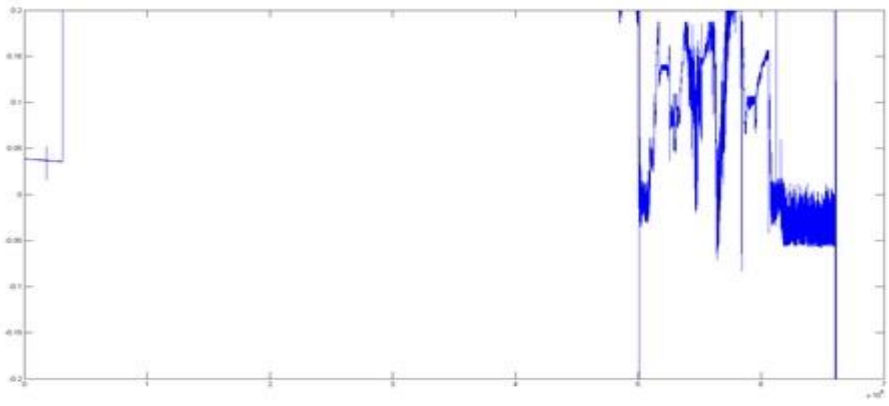

Figure 6.1: Saturated EEG signal from conventional electrode due to insufficient skin prep in one subject (#12)

The shelf life of pre-gelled Ag/ AgCl electrodes is about a month once the package is opened [6-1]. Using electrodes from pouches that were opened more than a month earlier, may not be a good experimental practice.

The reliability and consistency of the EEG recorder should be thoroughly tested. In two instances, one of the EEG recorders did not record for the entire duration of the night.

One more source of error is that the gold (epidermal) electrodes are very neutral and thus can accumulate charge, leading to DC drift. This, in comparison to conventional Ag/ AgCl electrodes, gives rise to a lot more drift based on empirical evidence and can be a challenge. Having a silver material based epidermal electrode might overcome the problem.

6.2 Future directions

As of now, the comparison between the two electrode technologies has been done only at the input EEG power feature level. Comparison of epidermal and conventional electrodes at the remaining levels, such as using KL divergence to compare the two sets of parameter values $\theta = \{\pi, Q, R\}$ or comparing the MAP sequence estimate outputs (hypnograms) are steps in the future direction. Another step will be to validate both the EEG data with the help of an expert clinician (somnologist) and also to validate the algorithm using available online datasets such as the Physionet. We also intend to extract EOG and EMG signals from the existing single-channel EEG for validating the duration of specific sleep stages based on the changes in EOG and EMG. An all forehead montage of recording, reference and ground will also be tested for less obtrusive studies with epidermal electronics. In addition, a rigorous validation study comparing

Polysomnography (PSG) vs. epidermal electronics performed on a number of subjects as supported by statistical power calculations is part of the future steps to be taken.

6.3 Potential Impact

Abnormal sleep patterns are inherently linked to impending neurodegenerative disorders. Ideally, if people can take home a portable sleep recording device that is easy – to – wear, it can be used to record sleep on a day-to-day basis. Having a regularly monitored sleep data every single night makes it more plausible to have enough data to compare and come up with objective markers of disorders that have serious ties with sleep. Markers of PTSD, predictions of drugs used for depression treatment and early diagnosis of Alzheimer's disease before clinical symptoms come to the surface could possibly be detected.

Figure 6.2: Futuristic wireless single-channel EEG based unobtrusive, seamless sleep monitoring device

REFERENCES

[1-1] Stranges, S., Tigbe, W., Gómez-Olivé, F. X., Thorogood, M., & Kandala, N. B. (2012). Sleep problems: an emerging global epidemic? Findings from the INDEPTH WHO-SAGE study among more than 40,000 older adults from 8 countries across Africa and Asia. Sleep, 35(8), 1173-1181.

[1-2] Pinholster, G. (2014, March 14). Sleep Deprivation Described as a Serious Public Health Problem Retrieved from http://www.aaas.org/news/sleep-deprivation-described-serious-public-health-problem.

[1-3] *9 Most Common Sleep Disorders*. Retrieved from http://health.howstuffworks.com/mental-health/sleep/disorders/9-most-common-sleep-disorders.htm.

[1-4] M.H. Kryger, T. Roth, and W. C. Dement, "Principles and Practice of Sleep Medicine 5Ed," Elsevier Saunders, (2010).

[1-5] Planes, C., D Ortho, M. P., Foucher, A., Berkani, M., Leroux, K., Essalhi, M., ... & Lofaso, F. (2003). Efficacy and cost of home-initiated auto-nCPAP versus conventional nCPAP. SLEEP-NEW YORK THEN WESTCHESTER-, 26(2), 156-160.

[1-6] Loredo JS, Clausen JL, Ancoli-Israel S, Dimsdale JE. Night-tonight arousal variability and interscorer reliability of arousal measurements. Sleep 1999;22:916-20.

[1-7] Drinnan MJ, Murray A, Griffiths CJ, Gibson GJ. Interobserver variability in recognizing arousal in respiratory sleep disorders. Am J Respir Crit Care Med 1998;158:358-62.

[1-8] Smith, J. R., & Karacan, I. (1971). EEG sleep stage scoring by an automatic hybrid system. Electroencephalography and Clinical Neurophysiology, 31(3), 231-237.

[2-1] Silber, M. H., Ancoli-Israel, S., Bonnet, M. H., Chokroverty, S., Grigg-Damberger, M. M., Hirshkowitz, M., & Iber, C. (2007). The visual scoring of sleep in adults. J Clin Sleep Med, 3(2), 121-131.

[2-2] *The different types of sleep*. Retrieved from http://thebrain.mcgill.ca/flash/d/d_11/d_11_p/d_11_p_cyc/d_11_p_cyc.html.

[2-3] Colten, H. R., & Altevogt, B. M. (Eds.). (2006). Sleep disorders and sleep deprivation: an unmet public health problem. National Academies Press.

[2-4] Squire, L. R. (Ed.). (2013). Fundamental neuroscience. Academic Press.

[2-5] Loomis, A. L., Harvey, E. N., & Hobart, G. A. (1937). Cerebral states during sleep, as studied by human brain potentials. Journal of experimental psychology, 21(2), 127.

[2-6] Retrieved from http://en.wikipedia.org/wiki/File:Stage2sleep.svg.

[2-7] Retrieved from http://perfotech.cereteth.gr/?p=1816. (this is going to be [2-5] - move accordingly.

[2-8] *Polysomnography*. Retrieved from http://en.wikipedia.org/wiki/Polysomnography.

[2-9] Kelly, J. M., Strecker, R. E., & Bianchi, M. T. (2012). Recent developments in home sleep-monitoring devices. ISRN neurology, 2012.

[2-10] Ancoli-Israel, S., Cole, R., Alessi, C., Chambers, M., Moorcroft, W., & Pollak, C. (2003). The role of actigraphy in the study of sleep and circadian rhythms. American Academy of Sleep Medicine Review Paper. Sleep, 26(3), 342-392.

[2-11] Shambroom, J. R., Fabregas, S. E., & Johnstone, J. (2012). Validation of an automated wireless system to monitor sleep in healthy adults. Journal of Sleep Research, 21(2), 221-230.

[2-12] Popovic, D., Khoo, M., & Westbrook, P. (2013). Automatic scoring of sleep stages and cortical arousals using two electrodes on the forehead: validation in healthy adults. Journal of sleep research.

[3-1] D.-H. Kim, N. Lu, R. Ma, Y.-S. Kim, R.-H. Kim, S. Wang, J. Wu, S.M. Won, H. Tao, A. Islam, K.J. Yu, T.-I. Kim, R. Chowdhury, M. Ying, L. Xu, M. Li, H.-J. Chung, H. Keum, M. McCormick, P. Liu, Y.-W. Zhang, F.G. Omenetto, Y. Huang, T. P. Coleman and J.A. Rogers, "Epidermal Electronics," Science 333 (2011): 838-843 (2011).

[3-2] *GS26 Pre-gelled Disposable sEMG Sensors - 150 pack*. Retrieved from http://bio-medical.com/products/gs26-pre-gelled-disposable-semg-sensors-150-pack.html.

[3-3] Ambu - Everyday Solutions in Cardiology Catalog. Retrieved from http://ambuusa.com/Files/Billeder/US/Catalogs/Animated%20Catalogs/Cardiology%20BiFold/files/assets/seo/page13.html.

[3-4] *Avatar EEG recorder*. Retrieved from http://webcache.googleusercontent.com/search?q=cache:http://avatareeg.com/productinfo.html.

[3-5] *3M Red Dot Trace Prep*. Retrieved from http://www.3m.com/product/information/Red-Dot-Trace-Prep.html.

[3-6] *Signa gel electrode gel*. Retrieved from http://www.parkerlabs.com/signagel.asp.

[3-7] Yao, D., Wang, L., Oostenveld, R., Nielsen, K. D., Arendt-Nielsen, L., & Chen, A. C. (2005). A comparative study of different references for EEG spectral mapping: the issue of the neutral reference and the use of the infinity reference. Physiological measurement, 26(3), 173.

[4-1] Luo, G., & Min, W. (2007). Subject-adaptive real-time sleep stage classification based on conditional random field. In AMIA Annual Symposium proceedings (Vol. 2007, p. 488). American Medical Informatics Association.

[4-2] Min, W., & Luo, G. (2009). Medical applications of EEG wave classification. Chance, 22(4), 14-20.

[4-3] Dumermuth, G., Lange, B., Lehmann, D., Meier, C. A., Dinkelmann, R., & Molinari, L. (1983). Spectral analysis of all-night sleep EEG in healthy adults. European neurology, 22(5), 322-339.

[4-4] Achermann, P. (2009). EEG analysis applied to sleep. Epileptologie, 26, 28-33.

[4-5] Bertsekas, D. P. (2002). Introduction to Probability: Dimitri P. Bertsekas and John N. Tsitsiklis. Athena scientific.

[4-6] Liu, Z., Huang, J., & Wang, Y. (1998, December). Classification TV programs based on audio information using hidden Markov model. In Multimedia Signal Processing, 1998 IEEE Second Workshop on (pp. 27-32). IEEE.

[4-7] Lo, C. C., Bartsch, R. P., & Ivanov, P. C. (2013). Asymmetry and basic pathways in sleep-stage transitions. EPL (Europhysics Letters), 102(1), 10008.

[4-8] Pan, S. T., Kuo, C. E., Zeng, J. H., & Liang, S. F. (2012). A transition-constrained discrete hidden Markov model for automatic sleep staging. Biomed. Eng. Online, 11, 52.

[4-9] Coleman, T.P. (2013, Spring Quarter), Statistics. BENG 100. Lecture conducted from University of California, San Diego, CA.

[4-10] *Maximum Likelihood*. Retieved from http://en.wikipedia.org/wiki/Maximum_likelihood.

[4-11] Coleman, T.P. (2008, July), Notes on Hidden Markov Models. Lecture conducted from University of Illinois, Urbana Champaign.

[4-12] Dempster, A. P., Laird, N. M., & Rubin, D. B. (1977). Maximum likelihood from incomplete data via the EM algorithm. Journal of the Royal statistical Society, 39(1), 1-38.

[4-13] Rabiner, L. (1989). A tutorial on hidden Markov models and selected applications in speech recognition. Proceedings of the IEEE, 77(2), 257-286

[4-14] Welch, L. R. (2003). Hidden Markov models and the Baum-Welch algorithm. IEEE Information Theory Society Newsletter, 53(4), 10-13.

[4-15] Coleman, T.P. (2013, Fall), Notes on Hidden Markov Models. Lecture conducted from University of California, San Diego, CA.

[4-16] Navidi, W. C. (2008). Statistics for engineers and scientists. McGraw-Hill Higher Education.

[4-17] *Non-parametric statistics*. Retrieved from http://en.wikipedia.org/wiki/Non-parametric_statistics.

[4-18] Efron, B., & Tibshirani, R. J. (1994). An introduction to the bootstrap (Vol. 57). CRC press.

[4-19] *Bootstrapping (statistics)*. Retrieved from http://en.wikipedia.org/wiki/Bootstrapping_(statistics)

[4-20] Lehmann, E. L., & Casella, G. (1998). Theory of point estimation (Vol. 31). Springer.

[4-21] *Covariance*. Retrieved from http://en.wikipedia.org/wiki/Covariance

[4-22] *Pearson product moment correlation coefficient.* Retrieved from http://en.wikipedia.org/wiki/Pearson_product-moment_correlation_coefficient

[6-1] Ambu Blue Sensor N specifications. Retrieved from http://webcache.googleusercontent.com/search?q=cache:kz_kIb4luEsJ:www.ambu.com/Admin/Public/Download.aspx%3FFile%3D/Files/Billeder/MediaDB/Originals/IE_N_493100301_V02_04121.pdf+&cd=2&hl=en&ct=clnk&gl=us